Doctoral Dissertation

Production and quality of recombinant IgA1 produced in disaccharide-adapted CHO-K1 cells

John Benson Dy Choa

March 2023

Laboratory of Applied Microbiology
International Center for Biotechnology

Department of Biotechnology
Graduate School of Engineering
Osaka University

DECLARATION

"I hereby declare that this dissertation is my original work and it has been written by me in its entirety. I have duly acknowledged all the sources of information which has been used in it. This dissertation has also not been submitted for any degree in university/institution previously."

.....

John Benson Choa

2023

Contents

List of Abbreviation

B4GalT	β-1,4-galactosyltransferase
B3GNT3	β-1,3-N-acetylglucosamiyltransferase 3
C1GalT1	N-acetylgalactosamine 3-β-galactosyltransferase
CBB	Coomassie Brilliant Blue
CHO-K1 cells	Chinese Hamster Ovary-K1 Cells
dIgA	Dimeric Immunoglobulin A
DTT	Dithiothreitol
ELISA	Enzyme-Linked Immunosorbent Assay
FBS	Fetal Bovine Serum
GalNT	N-acetylgalactosaminyltransferase
GalT	Galactosyltransferase
GAPDH	Glyceraldehyde-3-phosphate dehydrogenase
GCNT1	β-1,6-N-acetylglucosaminyltransferase
HMW	High Molecular Weight
FUT8	α-1,6-fucosytransferase
IgA1	Immunoglobulin A 1
IgA2	Immunoglobulin A 2
IgG	Immunoglobulin G
HC	Heavy Chain of Immunoglobulin
JC	Joining Chain of Immunoglobulins
LC	Light Chain of Immunoglobulin
LC-MS/MS	Liquid Chromatography- Tandam Mass Spectrometry
Man1	Mannosidase 1
Man2	Mannosidase 2
MGAT	α-1,3-Mannosyl-Glycoprotein 2-β-N-Acetylglucosaminyltransferase
OST	Oligosaccharyltransferase
pIgA	Polymeric Immunoglobulin A
pIgR	Polymeric Immunoglobulin Receptor

q_p	Specific Productivity
RP-HPLC	Reverse Phase- High Performance Liquid Chromatography
RT-qPCR	Real Time-quantitative Polymerase Chain Reaction
SiaT	Sialyltransferase
SDS-PAGE	Sodium Dodecyl Sulfate- Polyacrylamide Gel Electrophoresis
SEC-HPLC	Size Exclusion Chromatography- High Performance Liquid Chromatography
sIgA	Secretory Immunoglobulin A
ST3Gal	β-Galactoside-α-2,3-Sialyltransferase
ST6GalNAc	N-Acetylgalactoside-α-2,6-Sialyltransferase
TCEP HCl	Tris(2-carboxyethyl)phosphine Hydrochloride
rIgA	Recombinant Immunoglobulin A
PTM	Post-translational modification
UGGT1	UDP-glucose Glycoprotein Glucosyltransferase 1

List of Figures

List of Tables

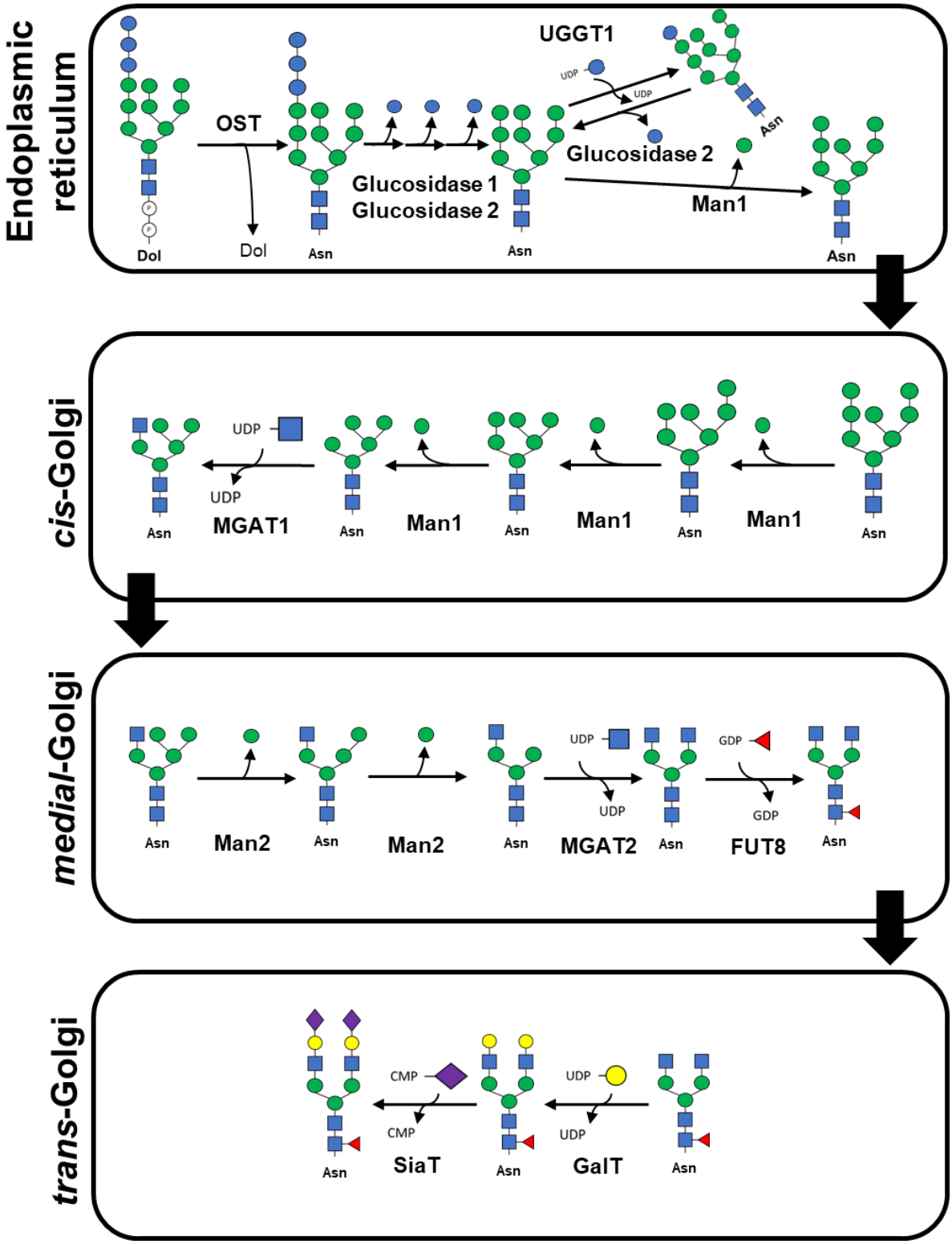

Figure 1 N-glycosylation pathway in mammalian cells. OST: Oligosaccharyltransferase, UGGT: UDP-glucose glycoprotein glycosyltransferase, Man 1: Mannosidase 1, MGAT 1: α-1,3-Mannosyl-Glycoprotein 2-β-N-Acetylglucosaminyltransferase 1, Man 2: Mannosidase 2, MGAT 2: α-1,3-Mannosyl-Glycoprotein 2-β-N-Acetylglucosaminyltransferase 2, FUT 8: Fucosyltransferase 8, GalT: Galactosyltransferase, SiaT, Sialyltransferase. Modeled from Essentials of Glycobiology 3rd edition.

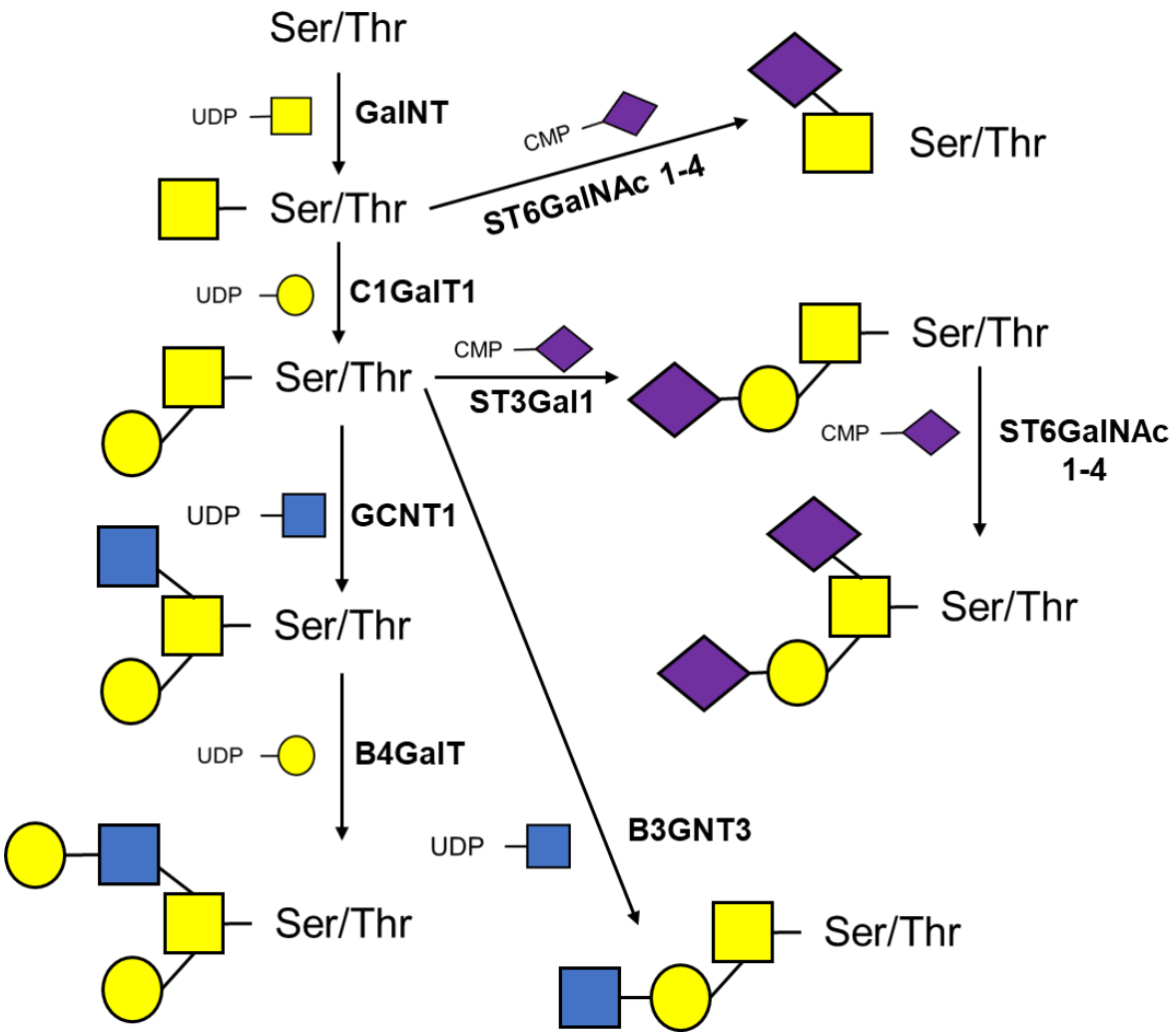

Figure 2 O-glycosylation pathway of mucin type O-glycan. GalNT: N-acetylgalactosamine transferase, C1GalT1: N-acetylgalactosamine 3-β-galactosyltransferase, ST6GalNAc 1-4: α-2,6-sialyltransferase 1-4, ST3Gal1: α-2,3-sialyltransferase 1, GCNT1: β-1,6-N-acetylglucosamine transferase, B4GalT: β-1,4-galactosyltransferase, B3GNT3: β-1,3-N-acetylglucosamiyltransferase 3. Modified from Essential of Glycobiology, 3rd edition.

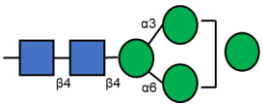

$Man_4GlcNAc_2$ (M4)

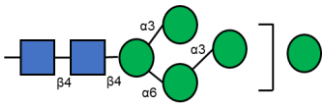

$Man_5GlcNAc_2$ (M5)

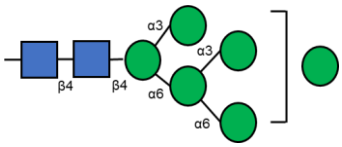

$Man_6GlcNAc_2$ (M6)

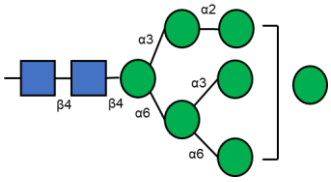

$Man_7GlcNAc_2$ (M7)

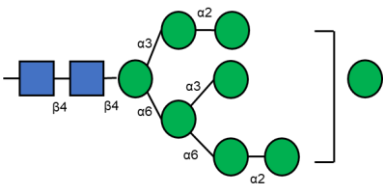

$Man_8GlcNAc_2$ (M8)

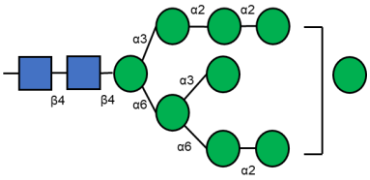

$Man_9GlcNAc_2$ (M9)

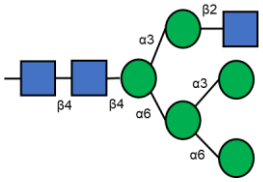

$GlcNAcMan_7GlcNAc_2$
(GNM5)

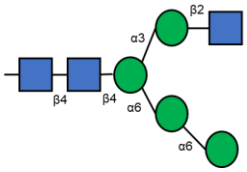

$GlcNAcMan_4GlcNAc_2$
(GNM4)

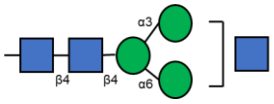

$GlcNAcMan_3GlcNAc_2$
(GNM3)

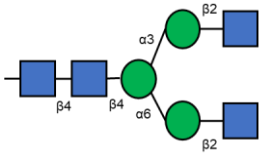

$GlcNAc_2Man_3GlcNAc_2$
(GN2M3)

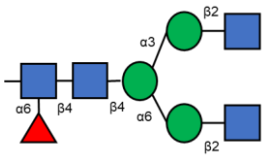

$GlcNAc_2Man_3(Fuc)GlcNAc_2$
(GN2M3F)

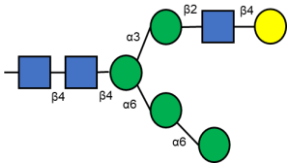

$GalGlcNAcMan_4GlcNAc_2$
(GalGNM4)

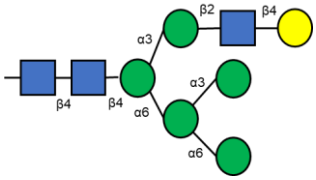

$GalGlcNAcMan_5GlcNAc_2$
(GalGNM5)

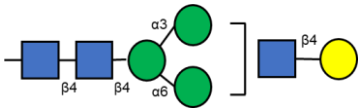

$GalGlcNAcMan_3GlcNAc_2$
(GalGNM3)

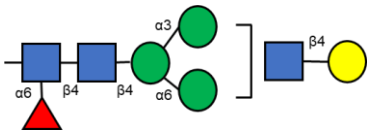

$GalGlcNAcMan_3(Fuc)GlcNAc_2$
(GalGNM3F)

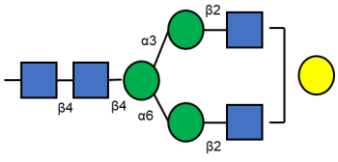

$GalGlcNAc_2Man_3GlcNAc_2$
(GalGN2M3)

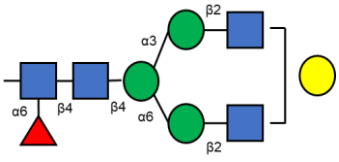

$GalGlcNAc_2Man_3(Fuc)GlcNAc_2$
(GalGN2M3F)

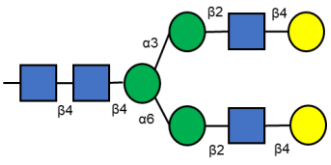

$Gal_2GlcNAc_2Man_3GlcNAc_2$
(Gal2GN2M3)

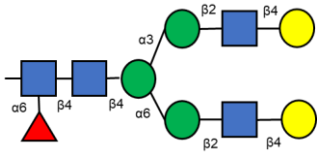

$Gal_2GlcNAc_2Man_3(Fuc)$
$GlcNAc_2$
(Gal2GN2M3F)

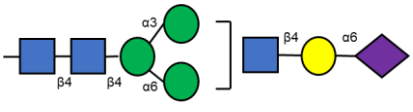

$SiaGalGlcNAcMan_3$
$GlcNAc_2$
(SiaGalGNM3)

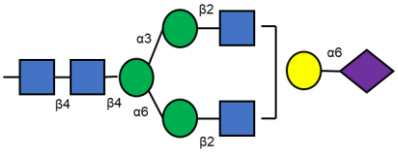

$SiaGalGlcNAc_2Man_3$
$GlcNAc_2$
(SiaGalGN2M3)

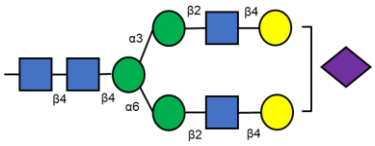

$SiaGal_2GlcNAc_2Man_3GlcNAc_2$
(SiaGal2GN2M3)

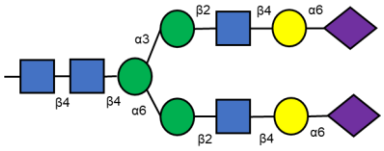

$Sia_2Gal_2GlcNAc_2Man_3GlcNAc_2$
(Sia2Gal2GN2M3)

Legend:

N-acetylglucosamine Galactose N-acetylneuraminic acid

Mannose Fucose

Figure 3 N-glycan structures found in recombinant IgA1 produced in CHO-K1 cells

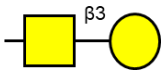

GalGalNAc
(Core 1 T antigen)

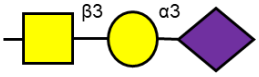

SiaGalGalNAc
(Sialyl-T antigen)

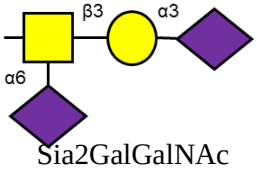

Sia2GalGalNAc
(Sialyl-Tn antigen)

Legend:

N-acetylgalactosamine Galactose N-acetylneuraminic acid

Figure 4 O-glycan structures found in recombinant IgA1 produced in CHO-K1 cells

Chapter 1 General Introduction

1.1 Mammalian cell lines as a robust platform for therapeutic protein production

The global biopharmaceutical industry is currently valued at $299 billion USD and is expected to grow in the future (*Global Biotechnology - Industry Data, Trends, Stats | IBISWorld*, n.d.). Most of the market shares are therapeutic protein produced by mammalian cell lines. Currently, there are various mammalian cell lines exist; however, Chinese hamster ovary (CHO) cells are the predominant cells that are used to produce these therapeutic proteins such as monoclonal antibodies and other life-saving biologicals. Eighty-nine percent (89%) of these therapeutic proteins are produced from CHO cells (Walsh & Walsh, 2022). Monoclonal antibody (mAb) production in CHO cells has advanced to the point where it can reach up to 10 g/L in fed-batch cultures (Kunert & Reinhart, 2016). Thus, making CHO cells the cell line of choice for recombinant protein production. Aside from this, post-translational modifications (PTM) are akin to humans, therefore, they are compatible and bioactive. In addition, CHO cells do not produce one of the immunogenic glycan epitopes, galactose-alpha 1,3-Gal (alpha-gal) which is found in other murine cell lines (Jenkins et al., 1996). In addition, different CHO cell lines have been developed to further improve recombinant protein production such as CHO DXB11 (*dhfr* +/-), CHO DG44 (*dhfr* -/-) and CHO-GS-/- (CHO-K1SV) (Tihanyi & Nyitray, 2020). These cell lines make cloning selection more time efficient by using metabolic markers dihydrofolate reductase-mediated methotrexate and glutamine synthetase-mediated methionine sulfoximine-based selection. In the year 2020, 12 out of 13 approved biopharmaceuticals by the US FDA were either monoclonal antibody or antibody-conjugates (Mullard, 2021). This just shows that antibodies will still be in demand for years to come.

1.2 Recombinant IgA as a new therapeutic antibody

Therapeutic antibodies are recombinant antibodies that are used for various medical conditions such as neutralizing pathogens, targeting cancer cells, or blocking certain receptors. Antibodies are composed of an antigen-binding fragment known as the Fab region for recognition of its target and a crystallizable fragment known as Fc region for its biological function (Pecetta et al., 2020). Immunoglobulin G (IgG) has been the general isotype used as the backbone for therapeutic antibodies. However, recent advances on other immunoglobulin isotypes such as immunoglobulin A (IgA) have paved a new way to utilize these immunoglobulins to our advantage. Recent studies showed that IgA can form dimers in the presence of a small protein called joining chain (JC) to improve its tumor killing activity (Lohse et al., 2011). Another study suggests that IgA's ability to be transported to the mucosal membrane as secreted IgA (sIgA) by the recognition of polymeric immunoglobulin receptor (pIgR) can provide protection on the mucosal surface against pathogens such as influenza, tuberculosis, and polio (Balu et al., 2011; Devudu Puligedda et al., 2020; Seibert et al., 2013). A recent study also suggested that IgA can neutralize influenza virus by binding of the Fab region to the hemagglutinin stalk and the IgA Fc glycan binding to the hemagglutinin receptor binding site, and polymeric IgA can increase avidity against influenza (Sano et al., 2021). In addition, IgA can bind toxins and allergens (Nakanishi et al., 2017; Sun et al., 1995). Lastly, monoclonal IgA have been able to block SARS-CoV2 spike angiotensin converting enzyme (ACE) interaction in the respiratory system (Ejemel et al., 2020).

1.3 Structure and biochemical characteristics of IgA

IgA is one of the five isotypes of antibody found in mammals. It is the 2nd most prevalent antibody in serum and most abundant in the mucosal surfaces of the body. An average human produces around 66 mg/kg of IgA per day (Leusen, 2015). IgA's heavy chains (HCs)

and light chains (LCs), like other immunoglobulins, are folded into several variable (V) and constant (C) domains, each encoded by a separate exon. There are four in the HC namely VH, Cα1, Cα2, Cα3 and two in the LC namely VL and CL (Sousa-Pereira & Woof, 2019). In humans, IgA is divided into 2 subclasses namely, IgA1 and IgA2. In the mammalian serum, there are only 5% of monomeric IgA and mostly are polymeric IgA (pIgA) found on the mucosal surface which are dimeric in nature (Virdi et al., 2016). Each domain has the distinctive "immunoglobulin fold," which consists of a 110 residue-sheet sandwich of anti-parallel strands arranged around a stabilizing internal disulfide bond (Woof & Russell, 2011). IgA1 has a proline-rich hinge region of 23 amino acids with nine potential O-glycosylation sites (Ser and Thr residues), three to five of which have been shown to be occupied in serum IgA1. IgA2 is not O-glycosylated and lacks this 13-amino acid hinge region (Royle et al., 2003). In addition, IgA is one of the two isotypes that is capable of covalently binding to J-chain to produce oligomers which gives it unique functions such as the ability to be transcytosed by the pIgR to the mucosal surface and allows robust binding to lower-affinity antigens through increased avidity (Matsumoto, 2022). During transcytosis of dimeric IgA (DIgA) into the mucosal surface by pIgR, a 5 Ig-like domain called the secretory component (SC) binds to the dimeric IgA forming sIgA (Woof & Russell, 2011).

The JC is a small polypeptide 15 kDa in size which is exclusively attached to IgA or IgM to create polymeric IgA (pIgA) or pentameric IgM respectively. The human JC contains eight cysteine residues, 2 of which forms disulfide bonds with either α- chains or μ- chains and the other 6 forms intrachain disulfide linkages (Johansen et al., 2001). In addition, JC contains an N-glycosylation site which is essential for dimerization and attachment to pIgR (Wormald & Sim, 2007). JC is not essential for polymer formation; however, it is important structure for transportation to the epithelial region of the body (Johansen et al., 2000).

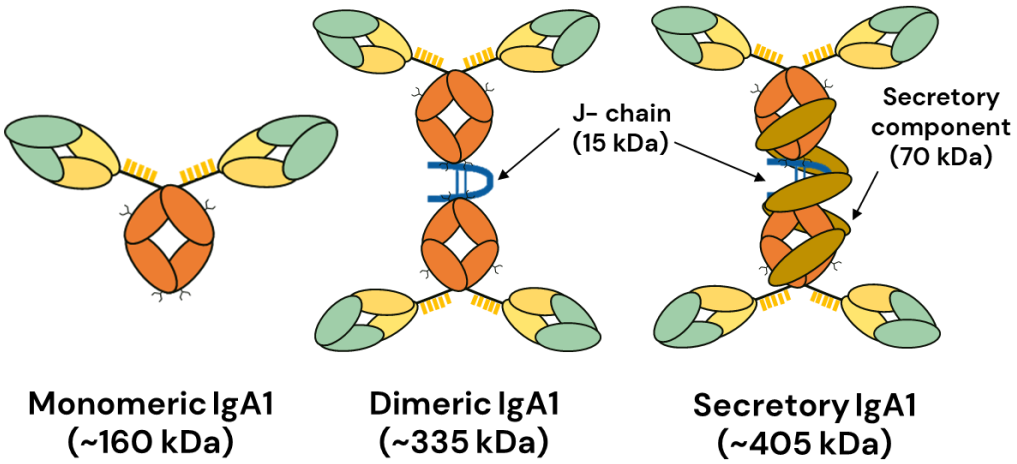

Figure 5 Structure of IgA1 monomer, IgA1 dimer, and secretory IgA1

1.4 N-glycosylation and O-glycosylation of IgA1

Glycosylation is a post translational modification in which saccharides are attached to proteins by enzymatic activity. Over 50% of all proteins are glycosylated and about 1-2% genes encode for glycan-related genes (Berger et al., 2011). There are 3 different types of glycosylation found in glycoproteins, N-glycosylation, O-glycosylation, and glycosaminoglycans. N-glycosylation are group of saccharides that form a glycosidic bond with asparagine residue via *N*-acetylglucosamine at conserve sequences Asn-XXX-Ser/Thr (X≠ Pro) while O-glycosylation are groups of saccharides that covalent bond with serine or threonine residues. Protein glycosylation can influence proper protein folding, cellular adhesion, cellular trafficking, receptor binding and activation (Marth & Grewal, 2008). IgA1 contains additional amino acids that are rich in proline, serine, and threonine in the hinge region which contains 6 to 10 O-glycosylation site that improves its flexibility which is not found in IgA2. IgA2 has additional N-glycosylation residues found in Asn166 of the constant region α1 (Cα1) domain and Asn337 of the constant region α2 (Cα2) domain (Sousa-Pereira & Woof, 2019). Both IgA subclasses contain an N-glycosylation found in the Cα2 chain and at the terminal constant region α3 (Cα3). IgAs are heavily glycosylated. In IgA1, glycosylation

accounts for 6-7% of its molecular weight while 8-10% for IgA2 (Woof & Ken, 2006). N-glycan structures found in the IgA1 of humans are mostly bisecting *N*-acetylglucosamine with sialic acid (Sia) and galactose (Gal) residues while N-glycan structures of IgA2 are found to be not only complex type, but also high-mannosylated-type and hybrid type were detected (Steffen et al., 2020). O-glycan structures of IgA1 found in humans are mostly mucin types with GalGalNAc forms disaccharide and its monosialylated and disialylated forms (Novak et al, 2000).

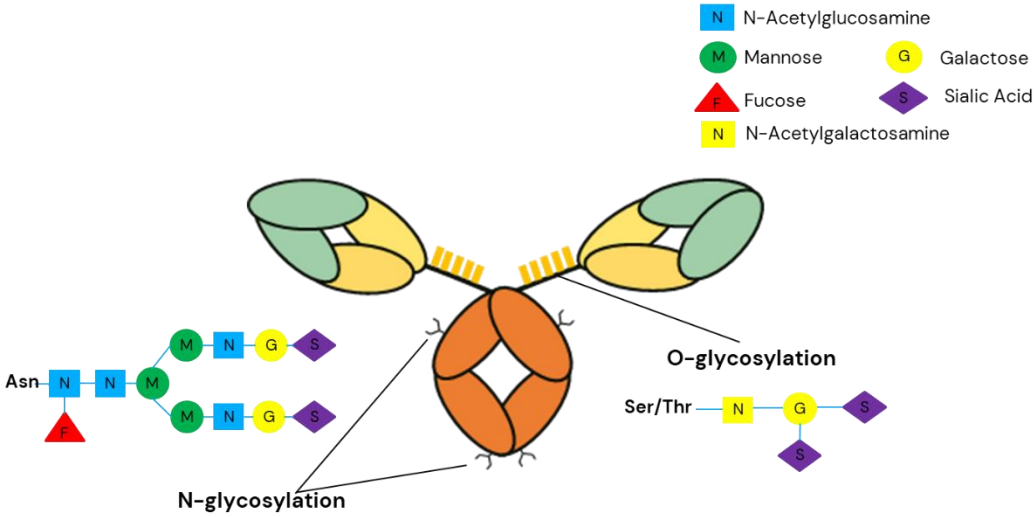

Figure 6 N-glycosylation and O-glycosylation of IgA1

1.5 Supplementation of disaccharides to improve recombinant protein production

Improvement on the production and quality of therapeutic antibodies has always been a necessity in the biopharmaceutical industry. Supplementation of the media is one of the simplest and most effective methods in improving the yield. Carbohydrate sources, especially glucose, has been used as an energy source for cell survival and growth. The ease of transportation via glucose transporter and sodium-glucose linked transporter has made it the standard source of sugar (Leong et al., 2017). However, high concentrations of glucose in media can increase lactate production and can cause toxicity to CHO cells (Leong et al., 2018). In a recent study, other monosaccharides such as galactose, fructose, and mannose were used

as an additional or a new source of carbohydrate for CHO cells to improve cell growth and viability (Ritacco et al., 2018).

Disaccharides are two monosaccharides that are bound together by a glycosidic bond. Common examples are sucrose, lactose, and maltose which are easily available and economical. Current studies suggest that disaccharides such as maltose and trehalose can improve recombinant IgG production and bi-specific antibody in CHO cells respectively (Leong et al., 2018; Onitsuka et al., 2014). In addition, N-glycosylation of recombinant IgG was changed when different sugars were supplemented to the media (Hossler et al., 2017; Leong et al., 2017).

1.6 Objectives of this study

This study aims to utilize various disaccharides namely, sucrose, maltose, lactose, and trehalose to improve the production and quality of recombinant IgA1 produced in serum-free CHO-K1 cells. For the first part of the study, stably producing rIgA1 CHO-K1 cells were adapted to high concentrations of disaccharides. After adaptation, the cell lines were upscaled to shaker flasks and the cell growth, cell viability, glucose consumption, lactate production, and rIgA1 concentration and specific productivity were analyzed to understand the effects on the rIgA1 produced in disaccharide-adapted CHO-K1 serum-free cell lines.

In the second part of the study, high molecular weight (HMW) aggregates, N-glycans, and O-glycans of recombinant IgA1 produced in disaccharide-adapted CHO-K1 cell lines were examined to see if HMWS of rIgA1 produced in the various cell lines were formed. N-glycans and O-glycans were also examined to observe changes on the N- and O-glycan profiles of the various cell lines.

Chapter 2 Production of recombinant IgA1 in disaccharide-adapted CHO-K1 cells

2.1 Introduction

Recombinant IgA possesses a distinct advantage compared to recombinant IgG which is the ability to be transcytosed to the mucosal membrane to provide protection against pathogens, allergens, and toxins (Devudu Puligedda et al., 2020; Ejemel et al., 2020; Nakanishi et al., 2017; Seibert et al., 2013; Balu et al., 2011 Sun et al., 1995). However, recombinant IgA production suffers from poor production yield (Reinhart & Kunert, 2015). Currently, there are no recombinant IgA on market even though it has numerous advantages. Therefore, there is a necessity to improve the productivity of recombinant IgA in mammalian cell lines.

In order to improve productivity on CHO cells, one of the most convenient methods is to modify the media composition. This study focuses on supplementation of different disaccharides to the media. Four different disaccharides namely sucrose, maltose, lactose, and trehalose were chosen because of their availability, and they are inexpensive reagents. In addition, few studies suggest that maltose and trehalose have been able to increase recombinant IgG and bi-specific antibody production respectively (Leong et al., 2018; Onitsuka et al., 2014). Currently, there is no study yet on how recombinant IgA1 production on CHO cells will be affected by the addition of these disaccharides. Thus, cell growth, cell viability, glucose consumption, lactate production, recombinant IgA1 specific productivity, and recombinant IgA1 aggregation will be observed and analyzed to determine if disaccharide addition will improve the recombinant IgA1 production.

2.2 Materials and Methods

2.2.1 Plasmid construction

DNA sequence of the IgA variable region was obtained from a hybridoma cell line established by fusion of immune cell from a dengue-infected volunteer in Thailand by SPYMEG technology conducted in the previous work (Sasaki et al., 2013). The following primers were used for cloning the variable region of the IgA: 5'-ATGAAACACCTGTGGTTCTTCCTCCT-3' (sense primer for amplification of the heavy chain), 5'-TGCACGTGAGGTTCGCTTCTGAACC-3' (anti-sense primer for amplification of the heavy chain), 5'-ATGGCCTGGWYYCCTCTCYTYCTS-3' (sense primer for amplification of the lambda chain) (W: A or T, Y: T or C, S: G or C), and 5'-TGGCAGCTGTAGCTTCTGTGGGACT-3' (anti-sense primer for amplification of the lambda chain). The amplified variable regions were ligated into pGEM®-T Easy vector (Promega, Wisconsin, USA). The IgA1 heavy chain and lambda chain constant region were synthesized by GeneArt™ gene synthesis service (ThermoFisher Scientific, Massachusetts, USA) based on DNA sequence from GenBank Accession ID AH007035.2 and JF806287.1 respectively. The heavy chain and lambda chain of variable regions and constant regions were inserted in pQCXIP (Takara Bio Inc. Shiga, Japan) and pQCXIH (Takara Bio Inc.) respectively to construct IgA1 expression vectors, pQCXIP-heavy chain and pQCXIH-light chain.

2.2.2 Construction of IgA1 stably producing CHO-K1 suspension cells

Stable transfection of CHO-K1 suspension cells was done by electroporation using Neon® transfection system (Thermo Fisher Scientific) following manufacturer's instruction. Briefly, CHO-K1 cells were seeded in 6-well plate 24 hours before electroporation. During the day of electroporation, cell density was counted, and approximately 1 x 10^6 cells/mL was collected. CHO-K1 cells were centrifuged at 400 x *g* for 5 minutes at room temperature and

washed with phosphate buffer saline (PBS) and centrifuged again at 400 x *g* for 5 minutes at room temperature. Cells were resuspended with resuspension buffer R to a final cell density of 2 x 10^7 cells/mL and mixed with 1.5 μg of pQCXIP-heavy chain and 1.5 μg of pQCXIH-light chain. The electroporation condition is as follows: voltage: 1150 V, width: 5 ms, pulse: 10. After electroporation, transfected cells were incubated at 37°C with 5% CO_2. After 24 hours post-transfection, 100 μg/mL hygromycin B (Fujifilm Wako Pure Chemical Corp., Osaka, Japan) and 1 μg/mL puromycin dihydrochloride dihydrate (Fujifilm Wako Pure Chemical Corp.) was added. Media and antibiotics were changed every 3 or 4 days for 21 days. Once the cell reached confluency, antibiotics were increased by 2-fold concentration until it reached 2 mg/mL Hygromycin B, and 20 μg/mL puromycin dihydrochloride dihydrate.

2.2.3 Cell line and cultivation

Serum-free CHO-K1 cells were subcultured using BMPro-W media (Funakoshi Corp., Tokyo, Japan) supplemented with 6 mM L-glutamine (Nacalai Tesque Inc., Kyoto, Japan) and incubated at 37°C with 5% CO_2. IgA1 stably producing CHO-K1 cell line were cultured using BMPro-W media supplemented with 6 mM of L-glutamine and 2 mg/mL hygromycin B and 20 μg/mL puromycin dihydrochloride dihydrate. Then, IgA1 stably producing CHO-K1 cells were adapted to 150 mM of different disaccharide stepwise, namely sucrose, maltose, lactose, and trehalose (Fujifilm Wako Pure Chemical Corp.). Briefly, IgA1 stably producing CHO-K1 cells were adapted to 50 mM of different disaccharides stepwise until disaccharide concentration reaches 150 mM. The cell growth was determined visually until confluency then subcultured with higher disaccharide concentration until it reached 150 mM of disaccharide.

2.2.4 Shake flask batch cultures sampling and evaluation

Approximately 3 x 10^5 cells/mL of non-adapted IgA1 producing CHO-K1 cells and disaccharide-adapted IgA1 producing CHO-K1 cells were seeded in a 50 mL baffled shaker

flask filled with 30 mL of media supplemented with 150 mM of disaccharide (sucrose, maltose, lactose, or trehalose) and incubated at 37°C with 5% CO_2 at 105 rpm. Samples were collected every 24 hours and checked for cell concentration and cell viability by trypan blue exclusion assay using TC20™ Automated Cell Counter (Bio-Rad Laboratories, California, USA). Specific growth rate was calculated using the formula:

$$\ln\left(\frac{VCD}{VCD_0}\right) = \mu t \quad (1)$$

Whereas: *VCD* = viable cell density end of log phase; VCD_0 = viable cell density start of log phase; μ = specific growth rate; t = time (days)

In addition, glucose consumption and lactate production were analyzed using BF-9 multi-use biosensor (Oji Scientific Instruments, Hyogo, Japan). After 9 days, samples from the media were collected for determination of IgA specific productivity as shown below and the remaining media were used to purify recombinant IgA.

2.2.5 Osmotic pressure measurement

Osmotic pressure was measured using Osmometer 3250 (Advanced Instruments, Inc. Massachusetts, USA). In brief, 250 µL of samples from the media of the different cell lines were transferred in the tube. Then, the reading was collected, and each sample was measured 3 times to obtain an accurate reading.

2.2.6 Recombinant IgA1 specific productivity by sandwich enzyme-linked immunosorbent assay (ELISA)

IgA1 specific productivity was assessed by sandwich ELISA. In brief, a 96-well microplate was coated with 5 µg/mL goat anti-human IgA (MBL Corp., Nagoya, Japan) capture antibody in 50 µL of PBS pH 7.4 and incubated at 4°C overnight. Capture antibody solution was removed, and the wells were washed with 200 µL wash buffer (0.05% Tween 20 in PBS)

three times. Wells were blocked with 1% BSA in wash buffer for 1.5 hours in room temperature. After washing three times, IgA standard purified from human serum (Bethyl Laboratories, Montgomery, TX, USA) at different concentration was introduced and collected media from non-adapted and disaccharide-adapted IgA1 producing CHO-K1 cell lines were added, and the plate was incubated for 1.5 hours at room temperature. Samples were discarded and washed with the same condition as above. Horseradish peroxidase (HRP)-conjugated goat anti-human IgA (MBL Corp.) at 1:6000 concentration was added and incubated for 1.5 hours at room temperature. After washing three times the same as above, 200 µL of Sigmafast *o*-phenylenediamine dihydrochloride (OPD) substrate (Sigma-aldrich, Missouri, USA) was added and incubated in the dark at room temperature for 12 mins. Reaction was stopped with 100 µL of 3 M HCl. The reaction was measured using iMARK™ microplate reader (Bio-Rad Laboratories) at 450 nm wavelength. Data was analyzed using microplate reader manager 6 using linear curve. IgA specific productivity was calculated using the formula:

First, the trapezium rule was used to calculate the integrated viable cell density (IVCD):

$$IVCD_t = IVCD_{t-1} + 0.5 \times (VCD_t + VCD_{t-1}) \times \Delta t \quad (2)$$

By plotting IgA1 concentration (P) against IVCD, specific IgA1 productivity was computed between two culture times:

$$q_p = (P_{t2} - P_{t1})/(IVCD_{t2} - IVCD_{t1}) \quad (3)$$

Tests were done in triplicates and standard error of mean (SEM) were used to calculate for the error bar.

2.2.10 Statistical analysis

All experimental data were collected in triplicates. Microsoft Excel was used for the statistical analysis. One-way ANOVA was used to compare the groups and Tukey's HSD test

was done the post-hoc test done to compare which groups have significant difference. $p<0.05$ value was considered having significant differences in the compared groups.

2.3 Results

2.3.1 Construction of IgA1 heavy chain and light chain expression vectors

The construction of expression vector is necessary to be able to produce recombinant IgA1 from CHO-K1 cells. In this study, 2 expression vectors were constructed pQCXIP-HC and pQCXIH-LC to carry the insert for IgA1 heavy chain and light chain respectively. IgA vHC was combined with IgA cHC and inserted inside the expression vector pQCXIP while IgA LC was inserted inside the expression vector pQCXIH (Figure 7). DNA sequencing was done to confirm the right insert sequence for the inserts.

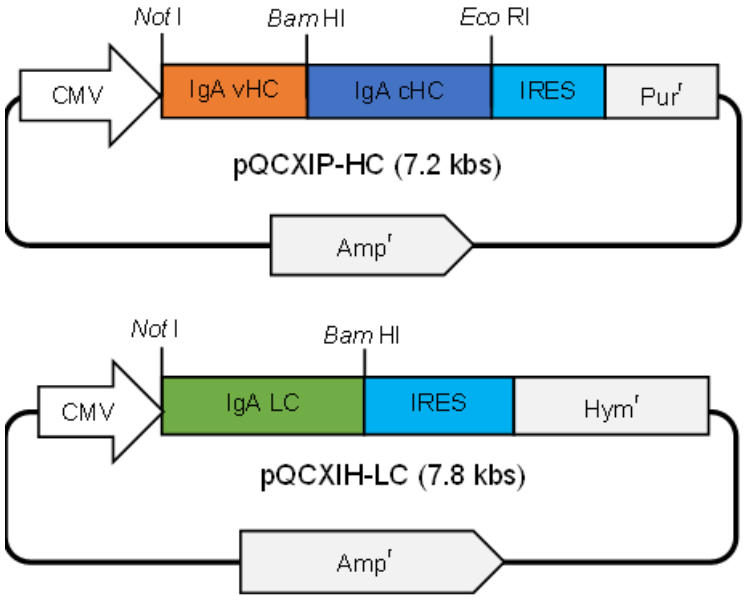

Figure 7 Vector construct for IgA1 Heavy Chain and Light Chain. CMV: Cytomegalovirus promoter, IgA vHC: IgA variable heavy chain region, IgA cHC: IgA heavy chain constant region, IRES: Internal ribosomal entry site, Pur^r: Puromycin resistance gene, Amp^r: Ampicillin resistance gene, IgA LC: IgA light chain, Hym^r: Hygromycin B resistance gene.

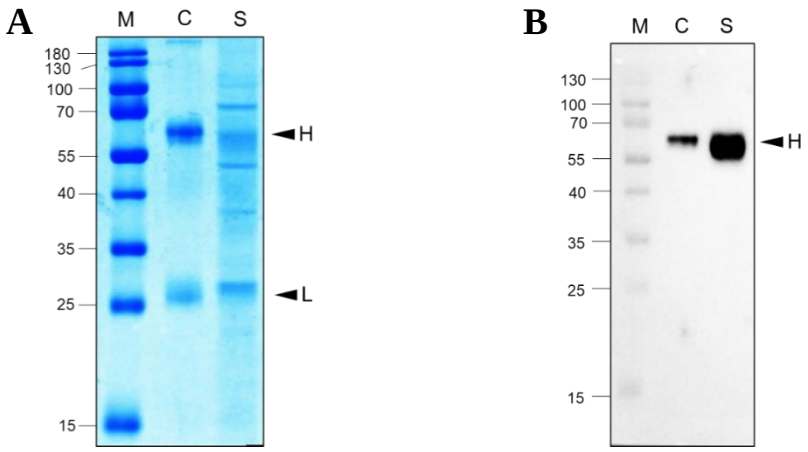

Figure 8 Recombinant IgA1 production in CHO-K1 suspension cells. (**A**) CBB of recombinant IgA produced in CHO-K1 suspension cells. (**B**) WB of recombinant IgA produced in CHO-K1 suspension cells. Antibody: HRP-conjugated goat anti-human (1:5000). IgA M: Marker, C: Standard IgA control, S: Supernatant fraction of CHO-K1 suspension cells.

After confirming the DNA sequences, the expression vectors were electroporated into CHO-K1 suspension cells using Neon® Electroporation System. Stable transfection was done by adding the antibiotics for 21 days then increased gradually until the cells can survive until 2 mg/mL of hygromycin B and 20 µg/mL of puromycin. IgA production was confirmed by CBB and WB. As seen in Figure 8A and 8B, presence of recombinant IgA1 was detected and the size was comparable to that of the IgA standard.

2.3.2 Cell growth, cell viability, glucose consumption, and lactate production

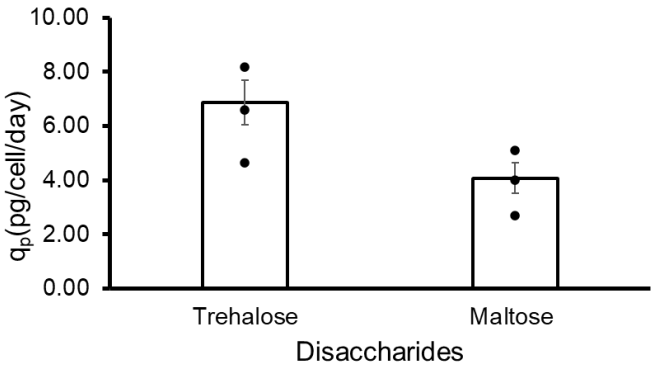

Figure 9 Specific productivity of 100 mM Trehalose- and Maltose-adapted CHO-K1 cell lines (N=3)

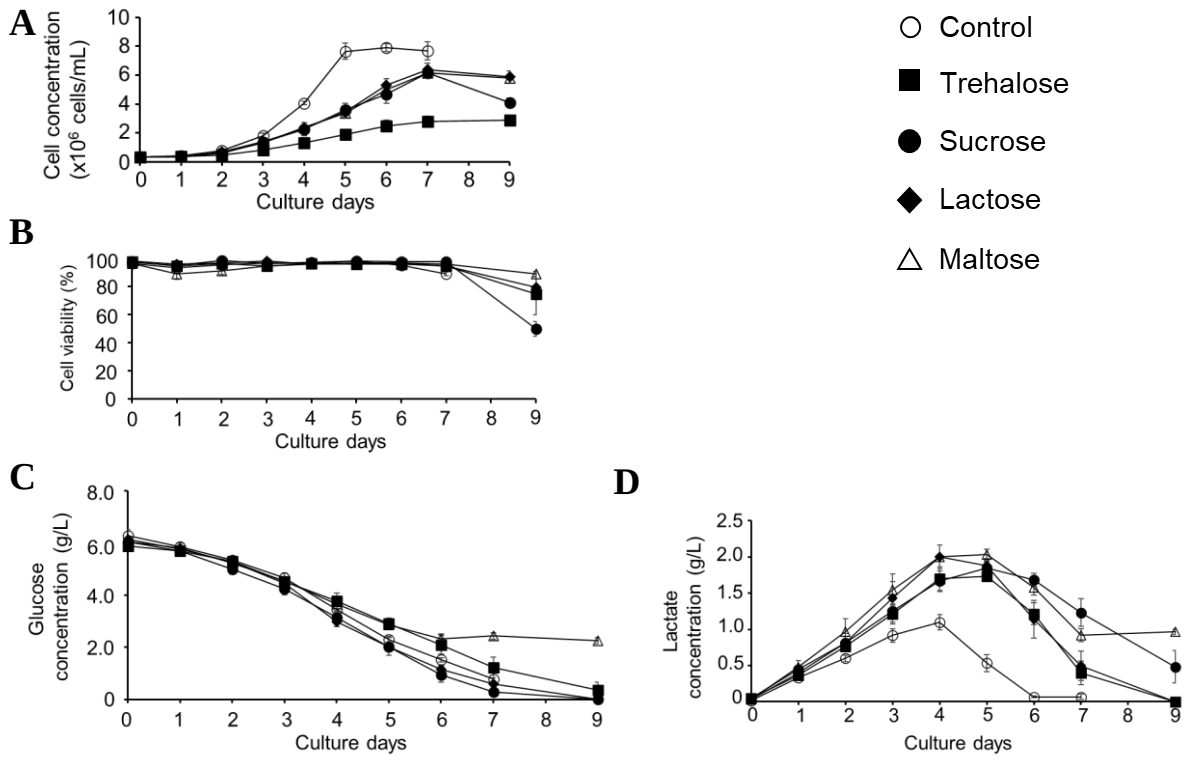

Figure 10 Effect of each disaccharide-adaptation on cell culture (N=3) (A) Cell concentration, (B) Cell viability, (C) Glucose consumption, (D) Lactate production, Control: non-adapted IgA producing CHO-K1 cells.

Table 1 Specific growth rate of non-adapted and disaccharide-adapted IgA1 producing CHO-K1 cell lines.

Cell lines	Specific Growth Rate (Day $^{-1}$)
Non-adapted cell line (Control)	0.72 ± 0.00
Sucrose-adapted cell line	0.39 ± 0.04
Maltose-adapted cell line	0.38 ± 0.01
Lactose-adapted cell line	0.38 ± 0.02
Trehalose-adapted cell line	0.21 ± 0.04

Table 2 Osmotic pressure of disaccharide supplemented media

Cell lines	mOsm/Kg
Nonadapted (Control)	297.7
150 mM Sucrose	456.7
150 mM Maltose	451.0
150 mM Trehalose	459.3
150 mM Lactose	452.0

Recombinant IgA1 producing CHO-K1 suspension cell lines were adapted to different disaccharides gradually at 50 mM until the cell lines can survive at 150 mM. cell lines were adapted to 100 mM of maltose and trehalose then productivity was analyzed. Indeed, specific productivity was increased (Figure 9). Therefore, we hypothesized that increasing the concentrations to 150 mM might give a higher productivity. Additionally, we used the same concentration as Onitsuka, et. al. 2014 in their previous experiment. Non-adapted IgA1 producing CHO-K1 cell line and 150 mM disaccharide-adapted IgA1 producing CHO-K1 cell lines were evaluated for the effects on cell growth, glucose consumption, lactate production. Cell concentration and viability of disaccharide-adapted IgA1 producing cell lines were compared with nonadapted IgA1 producing cell line. As shown in Figure 10A, the nonadapted cell line reached log phase earlier (5 days) compared to the disaccharide-adapted IgA1 producing cell lines (7 days). However, the nonadapted IgA1 producing cell line reached the death phase at a faster time at 7 days compared to the disaccharide-adapted cell line at 9 days. In addition, the maximum cell concentration for non-adapted cell line was higher compared to the disaccharide adapted cell lines reaching 7.92 x 10^6 cells/mL. While the highest cell concentration for the disaccharide-adapted cell lines was accounted for lactose-adapted IgA1 producing cell lines reaching 6.39 x 10^6 cells/mL which was the highest among the disaccharide

adapted cell lines. In contrast, trehalose-adapted IgA1 producing cell line tends to have the lowest cell concentration at 2.87 x 10^6 cells/mL compared to other cell lines. The cell viability among the cell lines is comparable starting from day 0 until day 7 where the non-adapted cell line starts to fall. Disaccharide-adapted IgA1 producing cell lines, especially maltose-adapted cell line, tends to have an extended cell viability at 89% even after 9 days of culturing (Figure 10B). Disaccharide-adapted IgA1 producing cell lines tended to have a slower growth rate compared to non-adapted IgA1 producing cell line (Table 1).

Cultivation of mammalian cells relies mostly on glucose as the carbohydrate source because of the ease of transport into the cells to be used as energy. Glucose consumption is a crucial parameter in the biochemical profiling because it is the primary energy source via aerobic glycolysis. Glucose concentration was measured daily until 9^{th} day. Nonadapted IgA1 producing cell line and disaccharide-adapted IgA1 producing cell lines except maltose-adapted IgA1 producing cell line have exhausted all the glucose over the end of cultivation time. Interestingly, maltose-adapted IgA1 producing cell line still contains 2.24 g/L of glucose at 9^{th} day of incubation (Figure 10C).

Lactate production is an important parameter to observe in cell cultivation for recombinant protein production because high lactate production can affect cell growth rate and cell viability negatively (Lao & Toth, 1997). Hence, high lactate concentration in the media can reduce recombinant protein productivity. In this study, lactate production was measured daily until 9^{th} day. During the 4^{th} and 5^{th} day of incubation, there was an observed increase in lactate production (Figure 10D). This can be attributed to Warburg effect in which cell preferred glucose as the source of ATP during the exponential phase (Rish et al., 2022). Increase in glucose metabolism can consequently increase the production of lactate. In addition, lactate production in disaccharide-adapted cell lines was higher than that in nonadapted cell

line. Interestingly, maltose-adapted cell line still contains higher lactate levels even after 9th day of incubation which was not seen in other cell lines.

These observed effects such as decreased cell concentration and slow growth rate are effect of cells cultured in hyperosmotic conditions. Thus, we measured the osmotic pressure of each cell lines. As seen in Table 2, all of the disaccharide-adapted cell lines have higher osmotic pressure compared to the nonadapted cell lines. Typically, normal osmotic pressure requirement for CHO-K1 cells must be below 300 mOsm/Kg (Romanova et al., 2022). However, when we add high concentrations of disaccharides, the osmotic pressure increase resulting in a hyperosmotic condition. At 150 mM of disaccharides, there is no little difference between the different disaccharides (Table 2).

2.3.3 Recombinant IgA1 production and specific productivity

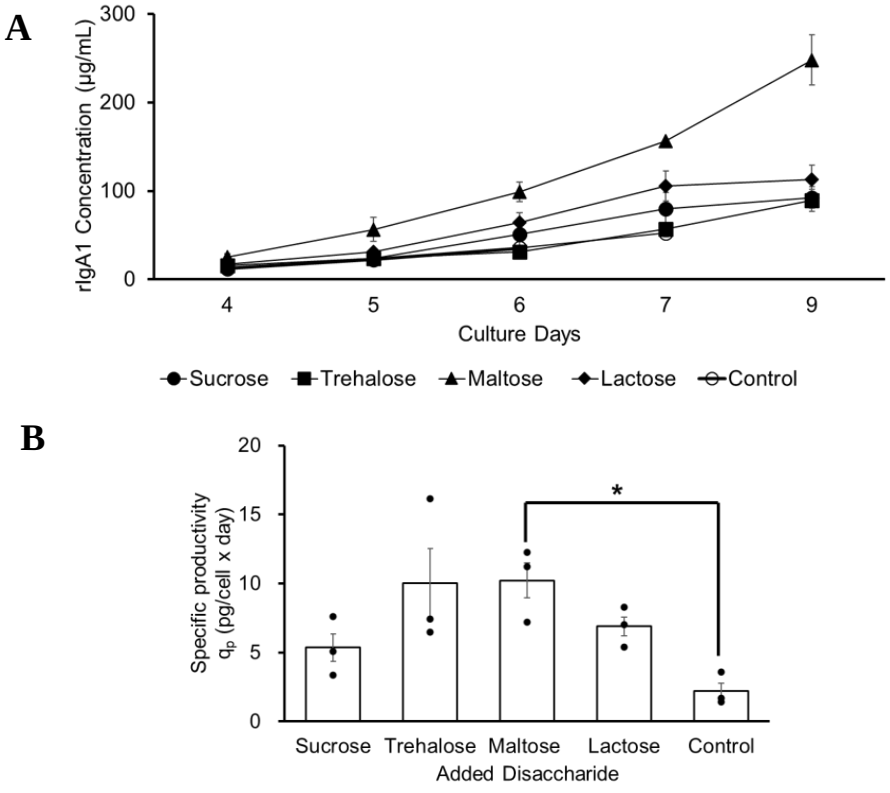

Figure 11 Recombinant IgA1 concentration and specific productivity of disaccharide-adapted and nonadapted IgA1 producing cell lines (**A**) Specific IgA1 productivity of disaccharide

adapted and nonadapted IgA1 producing cell lines (**B**). Control: nonadapted IgA1 producing CHO-K1 cells, N=3.

Sandwich ELISA was used to measure the cumulative and specific productivity of recombinant IgA1 produced in disaccharide-adapted and nonadapted IgA1 producing CHO-K1 cells. The samples were collected at 4^{th} day to 9^{th} day of subculturing. There was an observed increase in IgA1 productivity among all disaccharides-adapted cell lines compared to nonadapted cell line (Figure 11A). Maltose-adapted cell line showed the highest improvement in IgA1 production reaching 248 µg/mL at 9^{th} day of culture compared to nonadapted IgA1. In addition, specific productivity (q_p) of recombinant IgA1 of all the cell lines were calculated. The q_p of disaccharide-adapted cell lines were found to be higher compared to nonadapted cell line (Figure 11B). Among these disaccharide-adapted cell lines, maltose-adapted cell line and trehalose-adapted cell line showed the highest q_p at 10.2 pg/cell/day and 10.0 pg/cell/day respectively (Figure 9B). While nonadapted cell line only reached a q_p of 2.2 pg/cell/day. However, the high q_p of trehalose-adapted cell line did not reflect in the amount of recombinant IgA1 produced possibly because of the substantial decrease in the viable cells.

2.4 Discussion

IgAs have a distinct ability to provide protection to the mucosal membranes, neutralize pathogens with only their sugar chains that is not seen with IgG (Maurer et al., 2018). In order to utilize these advantages, we must first improve the yield. One of the most basic and effective methods is media supplementation. Transient addition of high concentrations of substances, on the other hand, may cause rapid osmotic changes in cells, which can be harmful (Han et al., 2010). Thus, in this study, we exposed recombinant IgA1 producing CHO-K1 cell lines to high concentrations (150 mM) of different disaccharides, namely sucrose, maltose, lactose, and trehalose, for an extended period until the cell lines could survive, and then measured cell growth, glucose consumption, lactate production, specific productivity, and aggregation.

First, nonadapted cell line reached a greater cell concentration compared to the disaccharide-adapted cell lines. In addition, specific growth rate of nonadapted cell line was higher compared to the disaccharide-adapted cell lines. Previous studies have shown that using NaCl to transiently apply hyperosmolarity also decrease cell concentration and specific growth rate (Kim and Lee 2002; Zhang et al. 2010; Kim et al. 2012), suggesting that the increase in osmolarity caused by disaccharides might also impose a similar osmotic pressure on cells as NaCl. However, even after nine days, compared to seven for the nonadapted line, the adapted cell lines still had higher cell viability. This might be due to the high osmolarity condition which is a consequence of supplementing the media with high concentrations of disaccharides. In addition, increase osmotic pressure can also affect the cell size (Kiehl et al., 2011). Glucose consumption analysis revealed that there is remaining glucose in the maltose-adapted IgA1 producing cell line, suggesting that maltose might have been utilized as another carbohydrate source. Indeed, a previous study presented the proof that maltose is utilized by CHO cells as a carbohydrate source (Leong et al., 2017, 2018). Lactate production was increased among disaccharide-adapted cell lines which can be attributed to an increase in osmotic pressure

caused by the addition of the different disaccharides thus activating Warburg effect (Moreira et al., 2021). However, a reducing in lactate production was seen during the stationary phase. According to a previous study, lactose dehydrogenase is the cause of this lactate inhibition (Omasa et al. 1992). Finally, specific productivity of recombinant IgA1 was improved, particularly with the maltose-adapted IgA producing cell line, which achieved specific productivity of 10.2 pg/cell/day of recombinant IgA compared to the non-adapted cell line, which had only 2.2 pg/cell/day. In comparison with other studies, this is the highest IgA1 specific productivity produced in CHO-K1 cells containing a lambda light chain (Reinhart & Kunert, 2015). This increase in productivity could be attributed to CHO cells being cultured in high osmolarity conditions and maltose utilization later in the cultivation process. Additionally, a previous study noted that the stationary phase of mammalian cell cultures showed an increase in recombinant protein production (Templeton et al., 2013). Hence, the further rise in recombinant IgA1 production may have been brought on by the stationary phase's extension, which can be observed in the growth curve of the disaccharide-adapted cell lines. These observed results are in agreement with other studies concerning cell cultures grown under hyperosmolarity condition (Kamachi & Omasa, 2018; Oh et al., 1993; Romanova et al., 2021).

Maltose has shown the most promising effect on productivity among these disaccharides whose effects on IgA1 production were investigated in this study because it has the combined effects of hyperosmolarity culture condition and an additional carbohydrate source for the later parts of cultivation. Furthermore, maltose is a cheap and readily available disaccharide. Clarifying how maltose is transported to cells and how maltose is metabolized is thought to increase the effectiveness of its addition even further. The specific effects and detailed mechanism of hyperosmolarity in CHO cells remain unknown. Previous research found that hyperosmolar cultivation increased mRNA expression of cell proliferation and cell cycle arrest genes, as well as cytosolic and mitochondrial ATP (Pfizenmaier et al., 2016).

Furthermore, proteomics analysis of IgG-expressing CHO cells cultured under hyperosmotic conditions revealed 23 proteins with variable expression, including increased expression of glyceraldehyde-3-phosphate dehydrogenase and pyruvate kinase, presumably to increase metabolic energy for antibody production (Lee et al., 2003). Another study found that when CHO cells were exposed to hyperosmolarity, their volume tripled and their mitochondrial activity increased (Romanova et al., 2021). Currently, there is little information on gene expression of transcription factors and signal transduction proteins under high osmotic pressure, it would be a useful method to establish host CHO-K1 cells that are tolerant to high osmotic pressure and capable of producing high target proteins from the standpoint of expression level control using RNA-seq and other methods.

2.5 Summary

Recombinant IgA have the potential to be an important new therapeutic antibody against mucosal infections, toxins, allergens, and tumors that recombinant IgG therapy cannot target. However, its consistently low yield production in mammalian cell lines makes development into a usable therapeutic antibody challenging. In this study, an improvement on the recombinant IgA production was done by adapting recombinant IgA1 producing CHO-K1 suspension cell lines to high concentration of various disaccharides namely sucrose, maltose, lactose, and trehalose. Maltose-adapted CHO-K1 cell lines have 4.5-fold increase in specific productivity in comparison with non-adapted cell line. This is also the highest specific productivity among the disaccharide-adapted cell lines. In addition, it is also the highest yield of recombinant IgA1 with a lambda light chain. The reason for this increase in recombinant IgA1 productivity might be the effect of high osmotic pressure from the addition of high concentrations of disaccharides. In addition, maltose might be utilized as additional carbohydrate source which improved cell viability for extended periods of culturing.

Chapter 3 Quality of recombinant IgA1 produced in disaccharide-adapted CHO-K1 cells

3.1 Introduction

Quality attributes of recombinant antibodies such as high molecular weight (HMW) aggregation and glycosylation is an important aspect in the production because it can influence the safety and efficacy. Aggregation of recombinant antibodies is known to be typically caused by incorrect association of LC and HC (Haberger et al., 2016). Aside from this, other factors such as imbalance ratio of HC to LC, Intracellular environments, and cell culture condition such as temperature and pH (Xu et al., 2022). Therefore, it is critical to evaluate aggregation in recombinant antibody production because substantial aggregated antibodies can trigger severe hypersensitive reactions and can be fatal (Rosenberg, 2006).

Glycosylation is an important post-translational modification (PTM) which affects the bioactivity, pharmacokinetics, immunogenicity, and safety of recombinant monoclonal antibodies produced. Glycosylated proteins are complex molecules, and even a well-controlled product can contain hundreds or thousands of glycoforms with the same amino acid sequence but different glycan composition (Schiestl et al., 2011). Manufacturers are required to produce consistent product that will produce the same efficacy and safety every time. For this reason, the analysis of the glycosylation profiles of recombinant antibodies is a necessary step.

IgA1 has 2 N-glycosylation sites found in the Cα2 and terminal Cα3 region and 3 to 5 O-glycosylation sites found in the hinge region (Figure 6). Previous studies have reported that N-glycosylation found on the C-terminal tail of IgA is capable of neutralizing influenza virus and other sialic acid-binding viruses (Maurer et al., 2018). Another study suggested that IgA1 and IgA2 in humans have different effects based on N-glycosylation they possess (Steffen et al., 2020). IgA1 contains more sialic acid reducing the affinity of Fc alpha Receptor (FcαR).

Thus, have less pro-inflammatory effect on neutrophils and macrophages compared to IgA2 (Steffen et al., 2020). Lastly, clearance of IgA is influenced by the amount of terminal galactose residues found in the O-glycosylation or N-glycosylation (Basset et al., 1999a). Aside from these, agalactosylated IgA O-glycosylation can cause IgA nephropathy (Novak et al., 2012). Thus, it is important to identify the different glycoforms that are present in recombinant IgA Because it might cause unwanted effects such as autoimmune disease.

Currently, there are numerous studies regarding the glycosylation of IgA in human serum because aberration in IgA glycosylation can cause diseases in human such as IgA nephropathy, Henoch-Schönlein purpura, and alcoholic cirrhosis (Allen et al., 1998; Suzuki & Novak, 2021; Tissandié et al., 2011). However, there are only a few studies concerning the recombinant IgA produced in different expression systems. One of the studies compared N-glycosylation of recombinant IgA produced in HEK293 and *N. benthamiana* (Göritzer et al., 2017). Another study compared the N-glycosylation of recombinant IgA1 and IgA2 in murine myeloma and CHO cell lines (Yoo et al., 2010). However, there is no study about N-glycan and O-glycan of recombinant IgA1 produced in CHO-K1 suspension cell lines under serum-free medium. Thus, in this study, N-glycosylation and O-glycosylation of recombinant IgA1 produced in CHO-K1 suspension cell line was analyzed. The effects of disaccharide-adaptation (sucrose, maltose, lactose, and trehalose) on the N-glycosylation and O-glycosylation of CHO-K1 suspension cell line was also analyzed. In addition, complete the investigation of the quality attributes of rIgA1, aggregation was also analyzed.

3.2 Materials and methods

3.2.1 Preparation of intracellular fraction

Using Cytobuster™ protein extraction reagent (Merck, Massachusetts, USA), the intracellular fractions of unadapted and maltose-adapted CHO-K1 suspension cells were obtained. Briefly, 1 mL of Cytobuster™ protein extraction reagent was added to cells wash with PBS. Then, incubated in room temperature for 5 mins. After, the samples were centrifuged at 15,000 x g for 5 mins. Lastly, the supernatant was collected and used for further experiments.

3.2.2 Recombinant IgA1 purification, western blot, and silver staining

Peptide M agarose (InvivoGen, California, USA) was used to purify recombinant IgA1 by following the manufacturer's instruction. Briefly, Peptide M agarose was equilibrated with 10 column volumes of equilibration and wash buffer (10 mM sodium phosphate, 150 mM NaCl, pH. 7.2). Then, samples were run through the column at a flow rate of 0.8 mL/min. After which the column was washed with the equilibration and wash buffer. Lastly, the 10 mL of elution buffer (0.1 M glycine, pH 2) was used to elute rIgA and immediately neutralized to pH 7 with neutralization buffer (0.75 M sodium phosphate pH 8.9). Then, purified IgA1 were mixed with 4x reducing SDS-PAGE buffer, and the samples were loaded in a 10% polyacrylamide gels to be separated under 100 V for 2 hrs. Then the separated IgA1 were transferred to polyvinylidene difluoride (PVDF) membrane (Immobilon-P, Merck) at 15 V for 25 mins. Next, the membrane was blocked with 1% skim milk for 1 hr. Washed with phosphate buffer saline- 0.5% Tween 20 (PBS-T) three times. The membrane was then incubated with HRP-conjugated goat anti-human IgA for 1 hr. Lastly, Silver staining was done using Silver Stain II Kit (Fujifilm Wako Chemicals Corp.) following manufacturer's instruction.

3.2.3 Recombinant IgA1 aggregation analysis

Amicon 10K Spin Column (Merck) was used to concentrate purified recombinant IgA1. The monomeric IgA1 and the aggregate IgA1 were then separated using Size Exclusion Chromatography High Performance Liquid Chromatography (SEC-HPLC). Briefly, 1 μg of purified recombinant IgA1 was injected into the HPLC system (Hitachi LaChrom L-7000, Tokyo, Japan) under the following conditions: TSKgel Ultra SW Aggregate 7.8 mm internal diameter (ID) x 30.0 cm (Tosoh Bioscience, Tokyo, Japan) UV wavelength at 280 nm, mobile phase 40 mM sodium phosphate buffer pH 6.7 containing 400 mM Sodium perchlorate at 0.3 mL/min for 60 mins. Column temperature at 25°C. The results collected was then interpreted as % aggregate and % monomeric IgA1.

Maltose-adapted cell line produced purified recombinant IgA1 was used to assess the effects of reducing agents on the disulfide formation in monomeric IgA1. Various concentrations of dithiothreitol (DTT) (Nacalai Tesque), Tris (2-carboethyl) phosphine hydrochloride (TCEP HCl) (Fujifilm Wako Pure Chemical), Glutathione (Nacalai Tesque), Cystamine diHCl (Nacalai Tesque) were added with the recombinant IgA1 at 37°C for 1 hr and run under non-reducing SDS-PAGE.

3.2.4 Recombinant IgA1 N-glycan and O-glycan sample preparation and 2-PA labeling

Purified recombinant IgA1 was dialyzed in deionized water overnight and N-glycans were digested using peptide-N-Glycosidase F (Takara®-Bio Corp.) according to manufacturer's instructions at 37°C for 24 hours. After digestion, the released N-glycans were separated using Amicon 10K spin column (Merck) from proteins and lyophilized. Hydrazinolysis was used to further digest the O-glycan fraction from the de-N-gylcosylated proteins for 6 hours at 60°C. After hydrazinolysis the sample was re-acetylated and run under

a strong cation exchange resin (Dowex-50x2 200 mesh) (Fujifilm Wako Pure Chemicals) and lyophilized. Both the N-glycan and the O-glycan were tagged with 2-aminopyridine (PA) reagent (Fujifilm Wako Pure Chemicals). In brief, 100 μL of 2-PA reagent was mixed with either N-glycan or O-glycan and incubated at 90°C for 1 hr. Dimethylamino borane, a reducing agent was added and incubated in 80°C for 40 mins and deionized water was added to stop the reaction.

3.2.5 N-glycosylation analysis by reverse phase-high performance liquid (RP-HPLC) chromatography

N-glycans were fractionated by reverse phase-high performance liquid chromatography (RP-HPLC) (Hitachi) under the following conditions, column: Cosmosil 5C18-AR-II 6.0 ID x 250 mm, solvent A: 0.02% trifluoroacetic acid (TFA)/milliQ water, solvent B: 0.02% TFA, 20% acetonitrile/milliQ water, flow rate at 1.2 mL/min, fluorescence detection at 310 nm for excitation and 380 nm for emission, run under gradient condition are as follows:

Solvent A:B= 100: 0% time: 0 min
Solvent A:B= 70: 30% time: 40 min
Solvent A:B= 100: 0% time: 41 min
Total run time: 50 min

3.2.6 O-glycosylation analysis by RP-HPLC

O-glycans were separated by RP-HPLC following the protocol (Rudd & Dwek, 2000) under the following conditions, column: Cosmosil 5C18-AR-II 6.0 ID x 250 mm, solvent A: 50 mM formic acid, adjusted to pH 5 with triethylamine, solvent B: 50% solvent A with 50% acetonitrile. The run condition are as follows:

Solvent A:B= 95: 5% time: 0-30 min	Flow rate: 0.5 mL/min
Solvent A:B= 80: 20% time: 31-161 min	Flow rate: 0.5 mL/min

Solvent A:B= 76: 24% time: 161-166 min Flow rate: 0.5 mL/min

Solvent A:B= 5: 95% time: 166-167 min Flow rate: 1.5 mL/min

Solvent A:B= 5: 95% time: 167-173 min Flow rate: 1.5 mL/min

Solvent A:B= 95: 5% time: 173-174 min Flow rate: 1.5 mL/min

Solvent A:B= 95: 5% time: 174-179 min Flow rate: 0.5 mL/min

Solvent A:B= 95: 5% time: 179-180 min Flow rate: 0.5 mL/min

Total run time: 180 min

3.2.7 Liquid Chromatography- Tandem mass spectrometry/mass spectrometry (LC-MS/MS)

The collected peaks were further analyzed by Liquid Chromatography- Mass Spectrometer/Mass Spectrometer (LC-MS/MS) (Agilent 1200 Infinity Series) (AmaZon ETD) subjected under the following conditions, column: Asahipak NH2P-50 2D 2.0 ID x 150 mm, solvent A: 2% AcOH/MeCN, solvent B: 5% AcOH, 3% TE/ milliQ water, flow rate at 0.2 mL/min, fluorescence detection at 310 nm for excitation and 380 nm for emission. The N-glycan run condition is as follows:

Solvent A:B= 80: 20% time: 0 min

Solvent A:B= 45: 55% time: 40 min

Solvent A:B= 80: 20% time: 41 min

Total run time: 50 mins

And the O-glycan run condition are as follows:

Solvent A:B= 95 :5% time: 0 min

Solvent A:B= 50 50% time: 40 min

Solvent A:B= 95: 5% time: 41 min

Total run time: 50 min

Collected LC-MS/MS data were analyzed using HyStar Post Processing (Bruker Daltonics). The N and O-glycan structures found were interpreted as percentages of relative abundance.

3.2.8 Reverse transcriptase real time quantitative polymerase chain reaction (RT-qPCR)

ISOGEN II (Nippon gene, Tokyo, Japan) was used to gather total mRNA from the various cell lines based on manufacturer's instruction. cDNA was created using Superscript IV VILO (Thermofisher Scientific) after total mRNA was obtained following manufacturer's instructions. Primer 3 and Primer-BLAST were used to create primers for the various sialyltransferases (ST3Gal1, ST3Gal2, ST3Gal3, ST3Gal4, ST3Gal6, ST6GalNAc4), α1,3-mannosyl-glycoprotein 2-β-N-acetylglucosamine transferase (MGAT1), and glyceraldehyde-3-phosphate dehydrogenase (GAPDH). Using SYBR gree.n master mix (Fujifilm Wako Pure Chemical Corp.), RT-qPCR analysis was performed on an Applied Biosystems™ Step One™ Real Time PCR system (Thermofisher Scientific). Using the ΔΔCt method, the relative expression of the selected genes was determined. The following formula was used:

$$\Delta\Delta\mathrm{Ct} = \Delta\mathrm{Ct}_{Sample} - \Delta\mathrm{Ct}_{Calibrator} \quad (1)$$

$$RQ = 2^{-\Delta\Delta Ct} \quad (2)$$

Normalization of data was done using nonadapted cell line which was used as the control for this experiment.

Table 3 List of Primers for RT-qPCR

Gene Name	Primer Pair (5'-3')
ST3Gal1	TCGTGGGAAACTCTGGGAAC GCCCTGTTCATCCTCACCAC
ST3Gal2	CCAGATTTACAACCCAGCCTTC AACCCATACACGTTCACCTCATC
ST3Gal3	CTCTTTGTCCTTGCTGGCTTC GACCCACGCACTCTTTCCTT
ST3Gal4	GAACAGCCCATCTTCCTCCA CATTCCCCACCACAACACA
ST3Gal6	CAGAGGAAGCCAGGAGAAGG GGTGGGATGGAAGTTGATGG
ST6GalNAc4	CATCTTCCTGTGCTATTGGGC CGGATAAGGGGCTTCCCATC

MGAT1	GAGCAACTGAGAGAAGCAAAGAAAG GGAAGAAGCCATGTACCAGACAG
GAPDH	GAGGACATCAAGAAGGTGGTGAA CAGCATCAAAGGTGGAAGAGTG

3.3 Results

3.3.1 Purification of recombinant IgA1

In this study, aggregation and glycosylation were analyzed to evaluate the quality attributes that is important for the production of recombinant IgA1. First, rIgA1 were purified by using peptide M. After purification, the rIgA1 were subjected to SEC-HPLC to assess the aggregation.

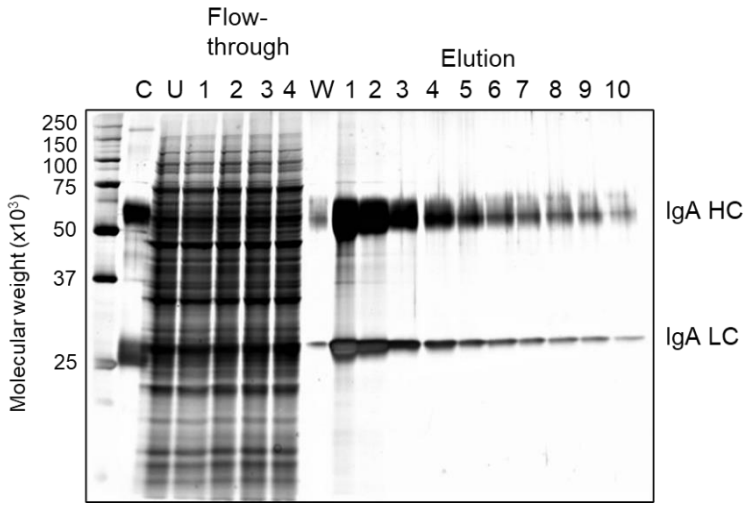

Figure 12 Silver staining of recombinant IgA1 purification using peptide M agarose. C: control monomeric IgA, U: unpurified media collected from IgA1 producing CHO-K1 cell line, W: Wash, IgA HC: Recombinant IgA1 heavy chain, IgA LC: Recombinant IgA1 light chain.

After collecting the media from the IgA1 producing CHO-K1 cell lines, purification was done using peptide M agarose and separated under 10% SDS-PAGE gel and then silver staining was done to assess the purity. The media were run through the purification column 4 times before washing. The flowthrough contained all the impurities and other proteins found in the unpurified fractions (Figure 12). However, the wash fractions contained recombinant IgA1 albeit in a negligible amount. The elution was collected every 1 mL to a total of 10 mL

to optimize the collection of the purified recombinant IgA1. As seen in Figure 12, elution fraction 1 to 4 contained the high concentration of purified IgA1. After which, the concentration begins to decrease. In addition, no impurities were seen in the elution fractions proving that peptide M agarose affinity purification is a simple and effective method for recombinant IgA1 purification.

3.3.2 Recombinant IgA1 Aggregation Analysis

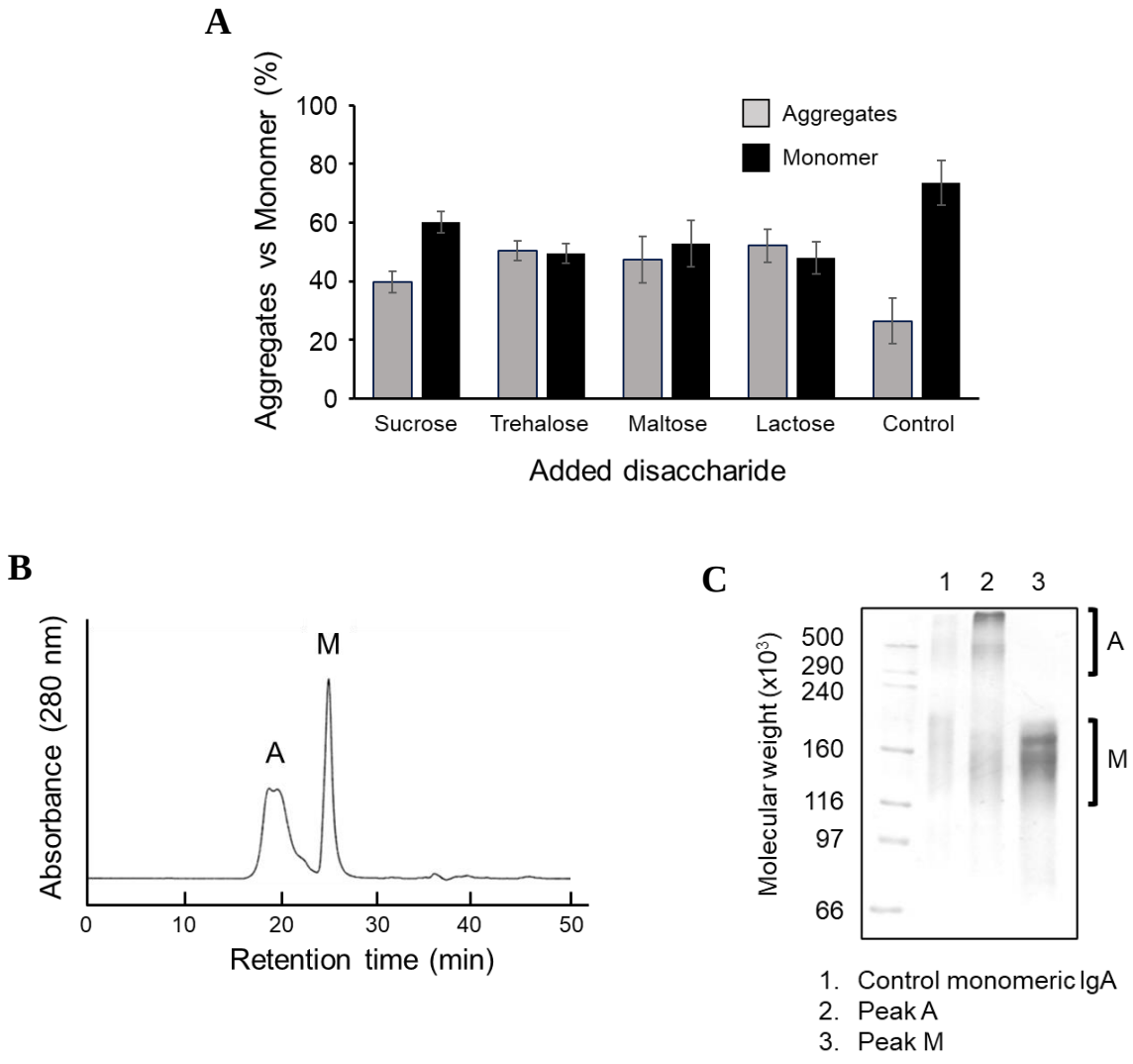

Figure 13 Effect of disaccharide addition on recombinant IgA1 HMW aggregation. (N=3) (**A**) Aggregated IgA1 vs Monomeric IgA1 separated using SEC-HPLC. (**B**) SEC-HPLC Chromatogram of maltose-adapted IgA producing cell line. (**C**) Coomassie Brilliant Blue

(CBB) staining of recombinant IgA1 separated by SDS-PAGE under non-reducing condition of collected peaks from SEC-HPLC. Control: non-adapted IgA producing CHO-K1 cells.

1: Control monomeric IgA standard, 2: Peak A in B, 3: Peak M in B. A: Aggregated IgA1, M: Monomeric IgA1

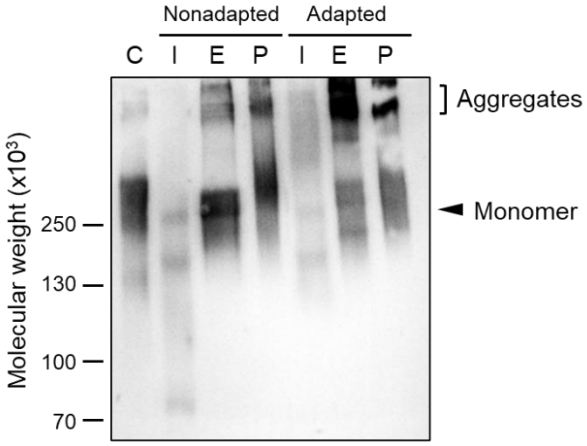

Figure 14 Investigation on the HMW aggregation of recombinant IgA1 produced in maltose-adapted and nonadapted CHO-K1 cell line. Western blot of intracellular fractions, supernatant fractions, and purified IgA1 from nonadapted cell line and maltose-adapted cell line separated by SDS-PAGE under non-reducing conditions C: Human IgA standard, I: Intracellular fraction, E: Extracellular fraction, P: Purified IgA1

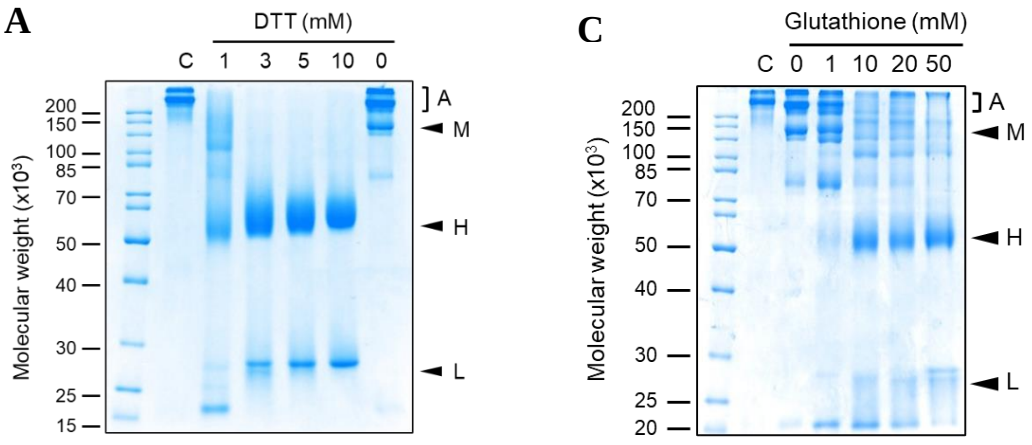

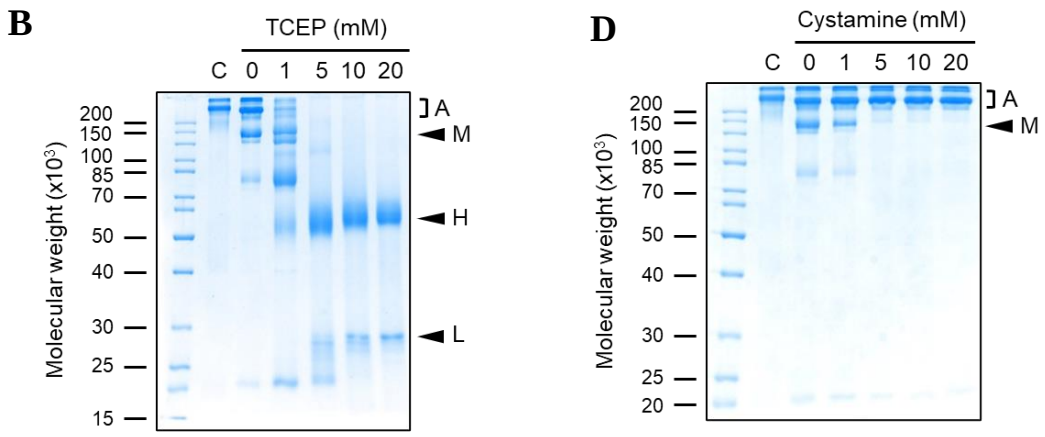

Figure 15 Coomassie Brilliant Blue staining of IgA1 purified from maltose-adapted cell line treated with non-treated IgA1 and separated by SDS-PAGE under non-reducing conditions (**A**) CBB of DTT in different concentrations (**B**) CBB of TCEP HCl in different concentrations. (**C**) CBB of Glutathione in different concentrations. (**D**) CBB of Cystamine diHCl in different concentrations. A: IgA1 aggregate, M: monomeric IgA1, H: IgA heavy chain, L: IgA light chain

Evaluation of HMW aggregation of recombinant antibody is a critical quality attribute in recombinant protein production. In this study, SEC-HPLC was done to assess the quality of recombinant IgA1 produced in disaccharide-adapted cell lines. Aggregation was present in all the recombinant IgA1 producing CHO-K1 cell lines. However, aggregation of recombinant IgA1 was found to be higher among disaccharide-adapted cell lines compared to non-adapted cell line (Figure 13A). To confirm the identity of the peaks in the SEC-HPLC, Individual peaks were collected. Then, the collected peaks were further separated under non-reducing SDS-PAGE. Peak A and Peak M from Figure 13B show the aggregated IgA1 and monomeric IgA1 respectively (Figure 13C). Past studies have shown that culturing CHO cells in hyperosmolarity conditions decrease recombinant antibody aggregation (Onitsuka et al., 2014; Qin et al., 2019). Our findings, however, demonstrated that IgA1 aggregation rose when the cell lines were grown in media with a higher osmolarity. The intracellular fraction, supernatant fraction, and

purified IgA1 of nonadapted and maltose-adapted cell lines were collected to ascertain when the IgA1 aggregation first started to develop. In Figure 14, while IgA1 aggregation is found in the intracellular fraction of maltose-adapted cell lines, it was absent from the intracellular fraction of nonadapted cell lines. The maltose-adapted cell line has more aggregated IgA1 than the nonadapted cell line in the supernatant fractions. Finally, compared to maltose-adapted cell lines, the purified IgA1 fraction of nonadapted cell lines still contained less aggregated IgA1. This finding demonstrates that the IgA1 aggregation started within the cells of the maltose-adapted cell line. According to a recent study, Cys-471 on the tailpiece of IgA has a predisposition to form self-aggregates when the J-chain is absent (Xie et al., 2021). Thus, various reducing agents, such as DTT, glutathione, TCEP hydrochloride, and cystamine dihydrochloride was used to reduce the disulfide bond formed by the presence of Cys-471 in order to see if the IgA1 produced exhibits the same behavior. IgA1 aggregates were indeed reduced when 1 mM DTT was added to isolated IgA1 from maltose-adapted cell line (Figure 15A). Higher DTT concentrations reduced all the disulfide linkages and caused the recombinant IgA1 to be divided into heavy chains and light chains (Figure 15A). In figure 15B, TCEP HCl, a tertiary phosphine and a known disulfide reducing agent, reduced the IgA1 aggregation at 1 mM. However, in higher concentrations it was found to reduce IgA1 into light chain and heavy chain. Next, Glutathione, a known reductant present in living organisms, decreased the amount of aggregated IgA1 at 1 mM and gradually reduced IgA1 into light and heavy chain with increasing concentrations (Figure 15C). Lastly, cystamine diHCl, an aminothiol that reacts with cysteine and is found in mammalian cells and is also used as a treatment against cystinosis (Xie et al., 2021), did not reduced the aggregation in any concentration (Figure 15D).

3.3.3 N-glycan analysis

N-glycan of recombinant antibodies is an important quality parameter because it can affect the bioactivity and metabolism of recombinant antibody. In this study, N-glycans were digested using PNGase F and tagged with 2-PA. then, RP-HPLC was used to separate the peaks and LC-MS/MS was used to identify the N-glycan structure of the collected peaks.

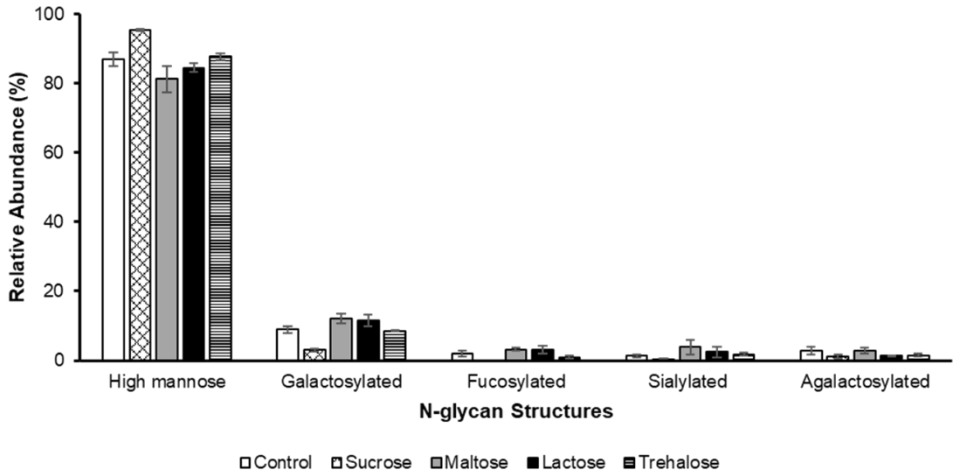

Figure 16 Relative abundance of different N-glycosylation groups on the different disaccharide-adapted cell lines (N=3). High mannose: terminal mannose containing N-glycan structures, Galactosylated: terminal galactose containing N-glycan structures, Fucosylated: fucose containing N-glycan structures, Sialylated: terminal sialic acid containing N-glycan structures.

Table 4 Relative abundance of N-glycan structures

	Recombinant IgA1 producing CHO-K1 cells				
		Disaccharide-adapted cells			
Structure	**Control**	**Sucrose**	**Maltose**	**Lactose**	**Trehalose**
M4	0.3 ± 0.2	0.2 ± 0.1	0.3 ± 0.2	1.8 ± 0.3	0.5 ± 0.2
M5	27.3 ± 3.2	10.9 ± 1.5	10.8 ± 4.5	25.3 ±8.1	13.0 ± 0.9
M6	42.1 ± 2.9	57.3 ± 3.0	43.1 ± 8.6	38.1 ± 5.8	48.8 ± 2.1
M7	12.0 ± 0.6	11.7 ± 0.7	13.9 ± 2.7	9.3 ± 2.4	13 ± 1.2

M8	2.8 ± 1.0	9.4 ± 0.9	7.1 ± 1.7	6.5 ± 0.7	6.4 ± 0.7
M9	2.6 ± 0.3	6.0 ± 0.9	6.1 ± 1.3	3.5 ± 0.8	6.2 ± 1.6
GNM3	0.8 ± 0.5	0.6 ± 0.2	1.5 ± 0.1	0.5 ± 0.2	0.8 ± 0.1
GN2M3	1.7 ± 1.3	0.2 ± 0.1	0.1 ± 0.1	0	0.2 ± 0.1
GN2M3F	0.2 ± 0.2	0	0	0	0
GNM5	0	0.5 ± 0.2	1.9 ± 0.8	1.5 ± 0.2	1.7 ± 0.1
GalGNM3	0	0.4 ± 0.2	0.3 ± 0.3	1.1 ± 0.5	1.4 ± 0.5
GalGNM3F	2.9 ± 0.9	1.2 ± 0.3	2.2 ± 0.5	2.4 ± 0.5	2.6 ± 0.3
GalGN2M3	0	0.2 ± 0.2	1.3 ± 0.8	0.8 ± 0.2	0.4 ± 0.1
GalGNM5	0	0	0	0.4 ± 0.3	0.2 ± 0.2
Gal2GN2M3	4.3 ± 0.4	1.6 ± 0.3	4.9 ± 0.5	4.1 ± 0.5	3.5 ± 0.1
GalGN2M3F	1.2 ± 0.5	0.2 ± 0.1	0.3 ± 0.2	0.2 ± 0.1	0
Gal2GN2M3F	0.5 ±0.3	0	2.6 ± 0.3	3.1 ± 0.7	0.9 ± 0.3
SiaGalGNM3	0	0	0.1 ± 0.1	0.8 ± 0.6	0
SiaGalGN2M3	0	0	0.5 ± 0.3	0	0.2 ± 0.1
SiaGal2GN2M3	1.3 ± 0.5	0	3.2 ± 1.2	1.6 ± 0.7	1.6 ± 0.3

Control: Nonadapted cells. ND= Not detected. N=3.

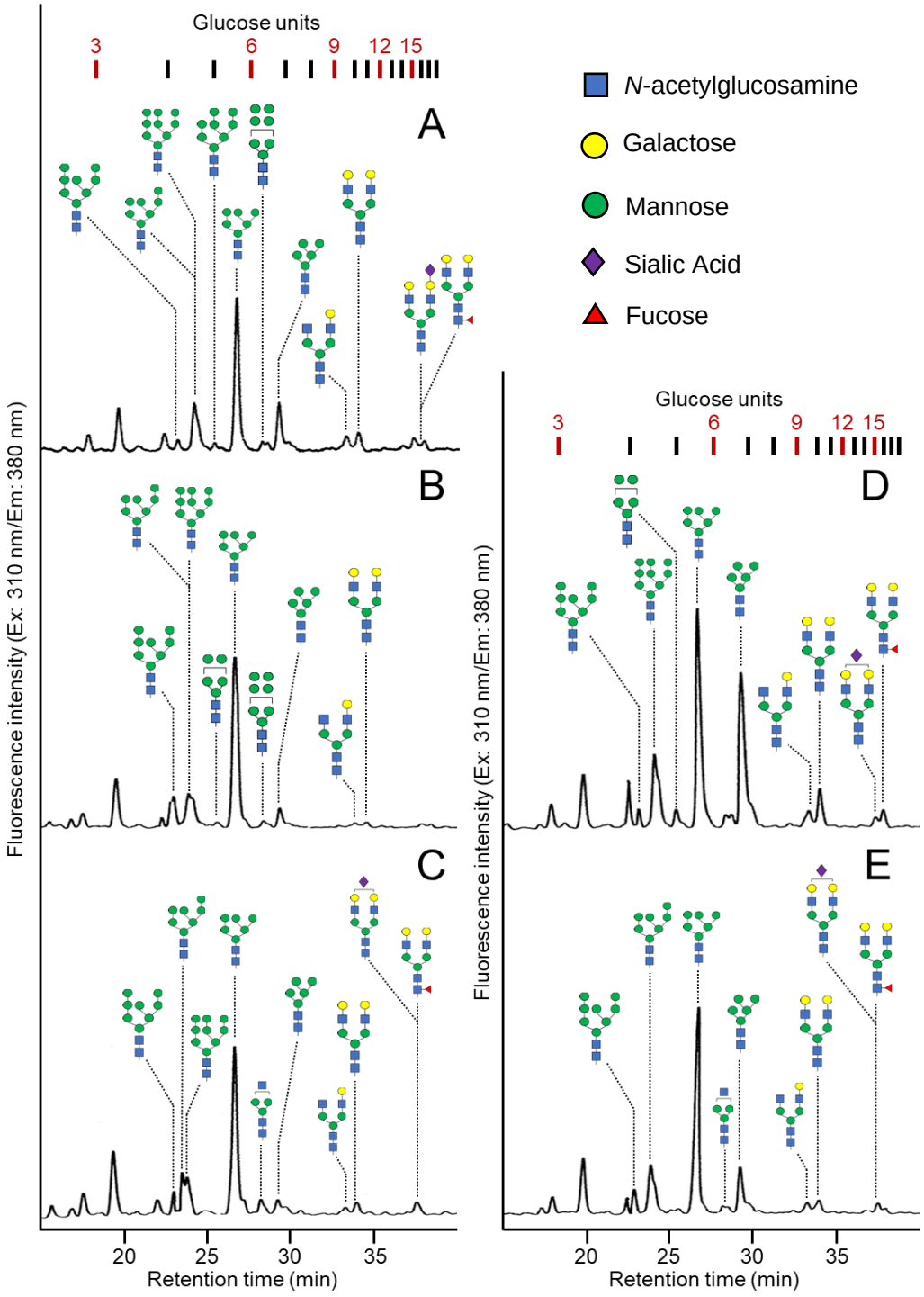

Figure 17 RP-HPLC chromatogram of the N-glycans with the corresponding structure derived from LC-MS/MS. (**A**) Nonadapted cell line, (**B**) Sucrose-adapted cell line, (**C**) Maltose-adapted cell line, (**D**) Lactose-adapted cell line, (**E**) Treha lose-adapted cell line

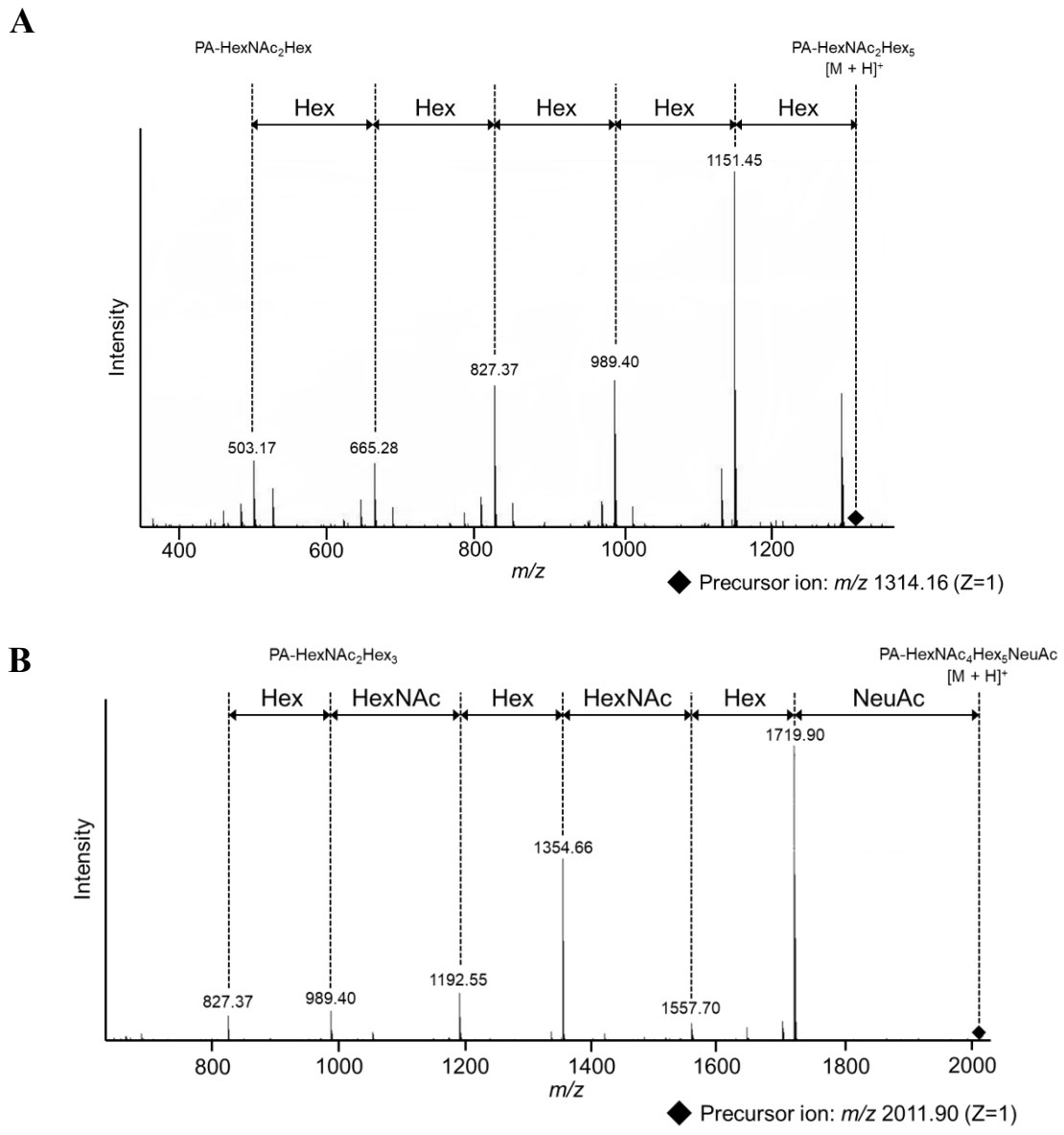

Figure 18 LC-MS/MS Spectogram of the different N-glycan types (**A**) High-mannosylated type N-glycan (M5), (**B**) Complex type N-glycan (SiaGal2GNM3)

The N-glycan profile is shown in Figure 16. Recombinant IgA produced by nonadapted IgA producing cell line contain mostly high-mannosylated N-glycosylation at 87% and galactosylated N-glycan at 9% also a few amounts of fucosylated N-glycan. Recombinant IgA produced by sucrose-adapted IgA producing cell line N-glycosylation are mostly high mannose at 95% and contain the lowest level of galactosylated N-glycan structure compared to other cell lines. In addition, there are no sialylated N-glycans detected in the sucrose-adapted cell

lines. Recombinant IgA1 produced by maltose-adapted IgA1 producing cell line contains 81% of high-mannosylated N-glycan and 12% of galactosylated N-glycan structure a few fucosylated and sialylated N-glycan. Recombinant IgA produced by lactose-adapted IgA producing cell line contains 85% high-mannosylated N-glycan and 12% galactosylated N-glycan. Recombinant IgA produced by trehalose adapted IgA producing cell line contains 88% high mannose N-glycan, 9% galactosylated N-glycan, a few fucosylated N-glycan, and sialylated N-glycan structures. The high-mannosylated N-glycans are mostly M5, M6, and M7 structures (Table 4). In addition to the summarized data on Figure 16, RP-HPLC peaks of N-glycans of the different rIgA1 producing disaccharide-adapted cell lines were matched with the N-glycan structures detected on LC-MS/MS of those respective peaks in Figure 17A to E. Different forms of high-mannosylated N-glycans were found (Figure 17A to E). Lastly, Figure 18A to B shows the LC-MS/MS spectrogram of high-mannosylated N-glycan structure (Figure 18A) and complex N-glycan structure (Figure 18B).

3.3.4 O-glycan analysis

Table 5 Relative abundance of different O-glycan structures

		Recombinant IgA1 producing CHO-K1 cells				
			Disaccharide-adapted cells			
Structure	**Number of experiment**	**Control**	**Sucrose**	**Maltose**	**Lactose**	**Trehalose**
GalGalNAc	1	ND	ND	ND	ND	ND
	2	54%	ND	ND	ND	ND
	3	ND	ND	ND	ND	ND
SiaGalGalNAc	1	ND	100%	74%	100%	83%
	2	46%	100%	46%	100%	100%
	3	ND	64%	100%	100%	100%
Sia2GalGalNAc	1	ND	ND	26%	ND	17%
	2	ND	ND	54%	ND	ND
	3	ND	36%	ND	ND	ND

Control: Nonadapted cells. ND: Not detected.

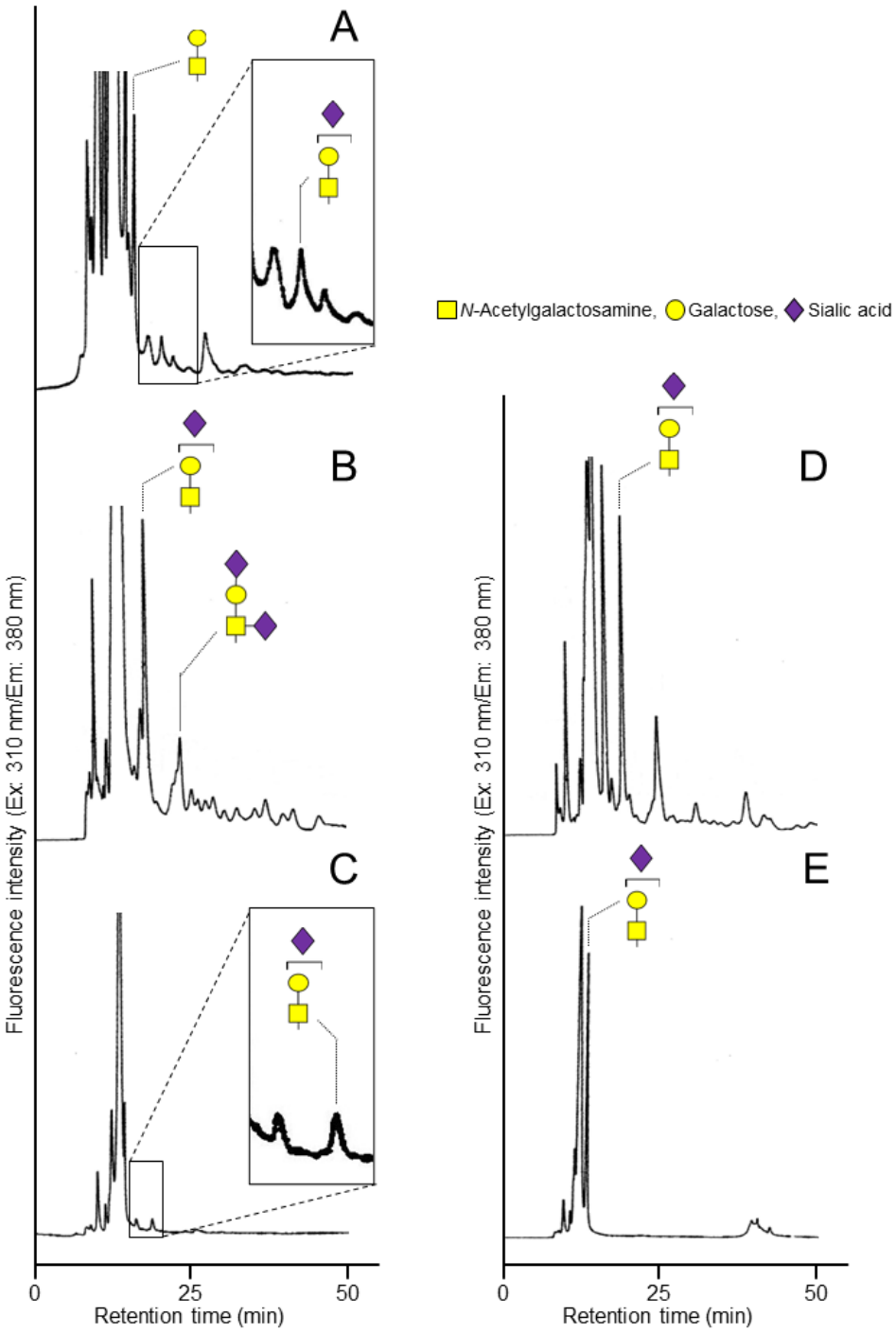

Figure 19 RP-HPLC chromatogram of the O-glycans with the corresponding structure derived from LC-MS/MS. (**A**) Nonadapted cell line, (**B**) Sucrose-adapted cell line, (**C**) Maltose-adapted cell line, (**D**) Lactose-adapted cell line, (**E**) Trehalose-adapted cell line

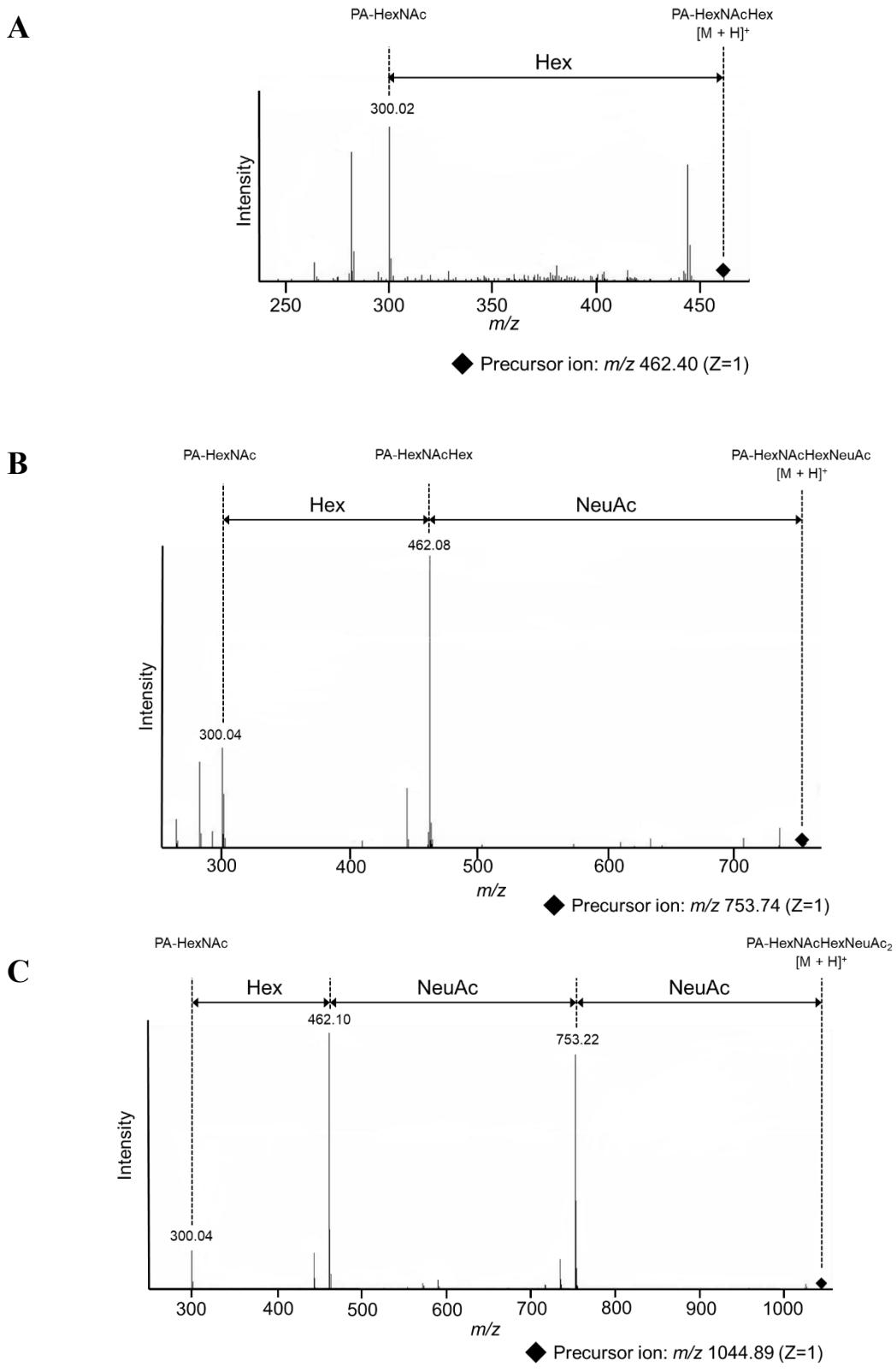

Figure 20 LC-MS/MS Spectogram of the different O-glycan types (**A**) GalGalNAc O-glycan, (**B**) SiaGalGalNAc O-glycan, (**C**) Sia2GalGalNAc O-glycan

O-glycan structures from different disaccharide-adapted IgA1 producing CHO-K1 suspension cell lines were analyzed. O-glycan profile are shown in Table 5. Recombinant IgA produced by nonadapted cell line was detected only in one of the three sample group it contains 54% of GalGalNAc structure and 46% of SiaGalGalNAc structures. Recombinant IgA1 from sucrose-adapted cell lines contains mostly of SiaGalGalNAc and Sia2GalGalNAc structures were detected only with one sample group. Recombinant IgA1 from maltose-adapted cell line contains both SiaGalGalNAc structures and Sia2GalGalNAc structures. In addition, maltose-adapted cell lines contain more of Sia2GalGalNAc structures compare to other cell lines. Recombinant IgA1 from Lactose-adapted cell line contain only SiaGalGalNAc O-glycan structures. Lastly, recombinant IgA1 from trehalose-adapted cell line contains mostly of SiaGalGalNAc structures and a few Sia2GalGalNAc structures. Interestingly, disaccharide-adapted cell lines lacked GalGalNAc O-glycan structures. In addition, Figure 19A to E shows the O-glycan structures corresponding to the RP-HPLC peaks in each of the rIgA1 collected from the different disaccharide-adapted cell lines. Lastly, Figure 20 A to C shows the different LC-MS/MS spectrograms of O-glycan structures collected from the different peaks found in RP-HPLC.

3.3.5 Relative gene expression levels of Sialyltransferases and MGAT1 on the different disaccharide adapted cell lines

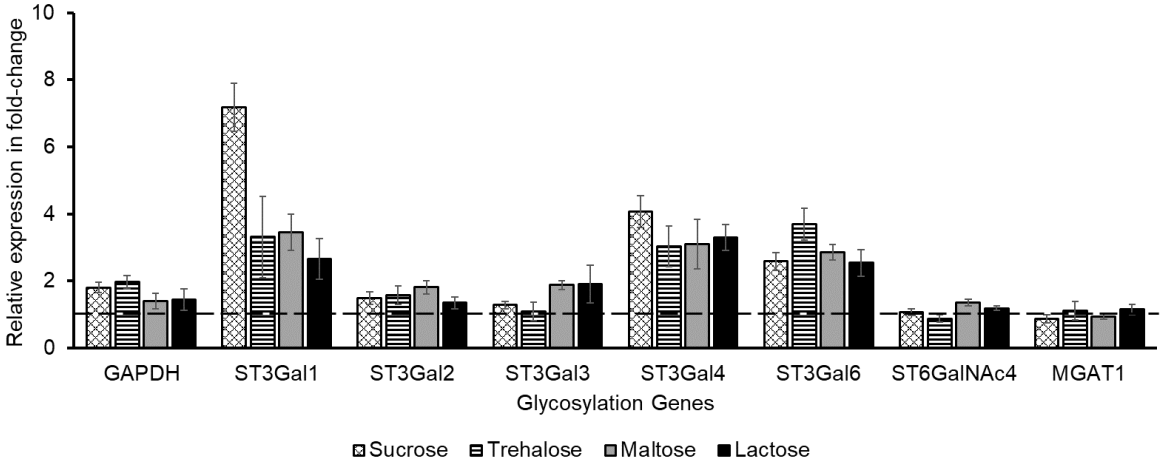

Figure 21 Relative gene expression of sialyltransferases and MGAT1 on the different disaccharide adapted cell lines. Broken line: Normalization was done using nonadapted cell line. (N=3)

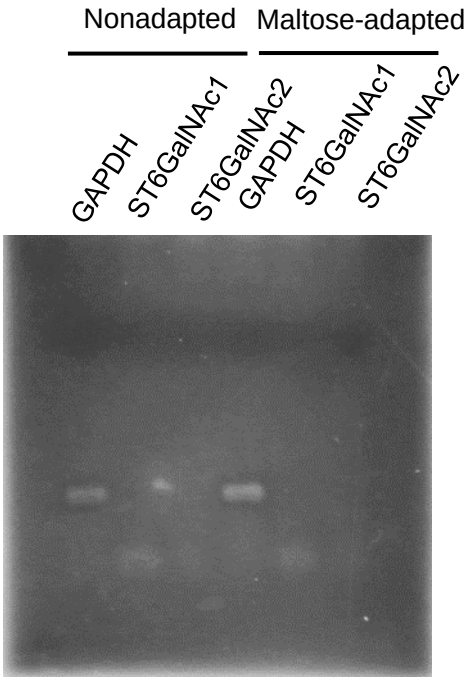

Figure 22 PCR of ST6GalNAc1 and St6GalNAc2 on cDNA of nonadapted and maltose-adapted cell lines. GAPDH as positive control

To identify the differences between the O-glycan structures observed in the various cell lines, the gene expression levels of the various sialyltransferases were examined. First, an

enzyme called CMP-N-Acetylneuraminate-α-galactosamide-alpha-2,3-sialyltransferase (ST3Gal) which transfers CMP-sialic acid to a substrate that contains galactose was analyzed. Indeed, in Figure 21, different disaccharide-adapted cell lines showed an increase of the ST3Gal 1 to 6 gene. Additionally, ST3Gal1, ST3Gal4, and ST3Gal6 have increased more significantly. As shown in Table 5 the SiaGalGalNAc O-glycan structure of the various disaccharide-adapted cell lines has increased, which is reflected in the increase in ST3Gal enzyme gene expression. Next, N-Acetylgalactosaminide α-2,6-Sialyltransferase (ST6GalNAc), an enzyme which catalyzes the addition of sialic acid to GalNAc residues was analyzed. The expression levels were unchanged among the nonadapted cell line and disaccharide-adapted cell lines. However, Sia2GalGalNAc structures were discovered in cell lines that had been adapted to sucrose, maltose, and trehalose in Table 4 In addition, in this study, ST6GalNAc4 was chosen as the enzyme because ST6GalNAc1 and ST6GalNAc2 cDNA are not detected (Fig 22). Lastly, A glycosylation enzyme called MGAT1 catalyzes the addition of UDP-N-acetylglucosamine to the mannose residue, which is crucial for the development of complex and hybrid N-glycan structures. The expression levels of MGAT1 in the nonadapted and disaccharide-adapted cell lines were unchanged (Figure 21).

3.3.4 Serum addition to recombinant IgA1 producing CHO-K1 cell suspension cell line

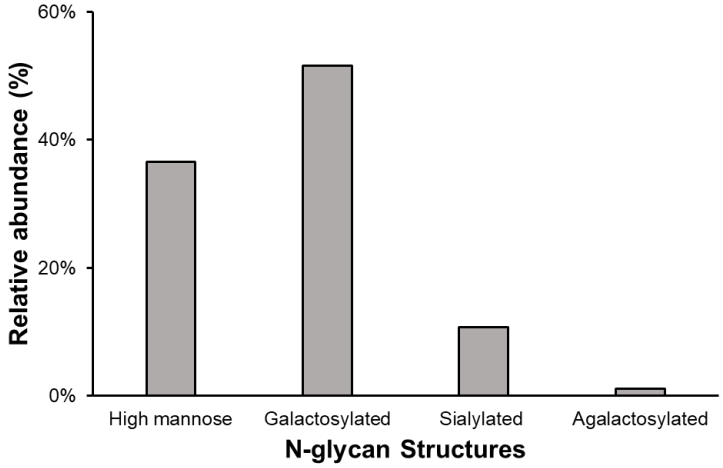

Figure 23 Relative abundance of different N-glycan groups on IgA1 producing CHO-K1 suspension cell lines cultured with 10% fetal bovine serum (N=2). High-mannosylated: terminal mannose containing N-glycan structures, Galactosylated: terminal galactose containing N-glycan structures, Fucosylated: fucose containing N-glycan structures, Sialylated: terminal sialic acid containing N-glycan structures.

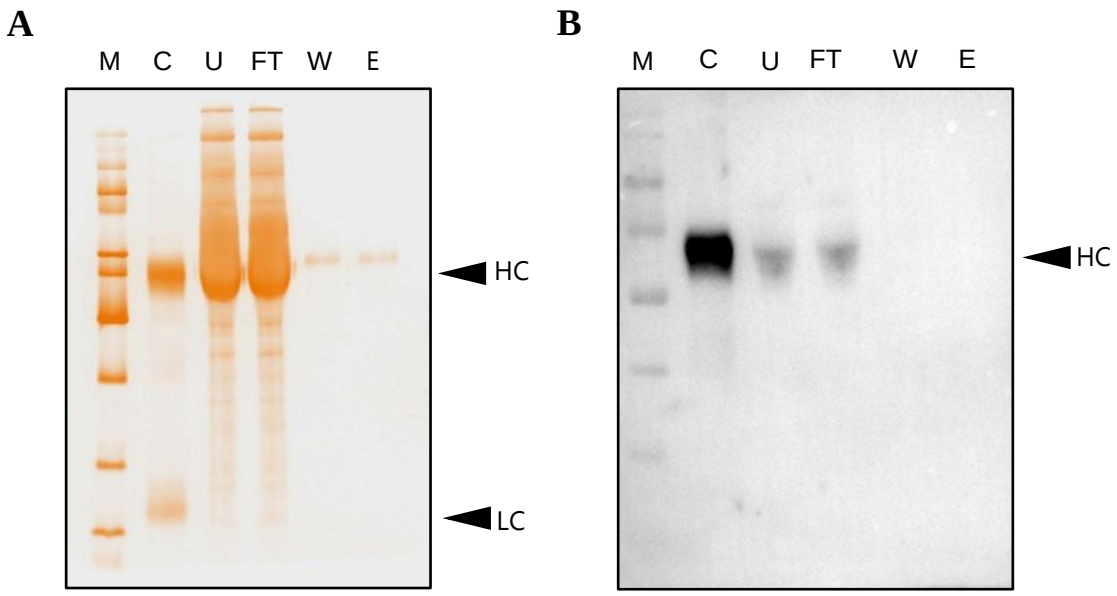

Figure 24 Purification of Ham's F12 media with 10% fetal bovine serum (FBS). (**A**) Silver staining of purified recombinant IgA1. (**B**) Western blotting of purified recombinant IgA1. M: Marker, C: Control (Human IgA standard), U: Unfiltered, W: Wash, E: Elution.

In this study, we found that recombinant IgA1 produced in serum-free cell lines produced significant amounts of high-mannosylated N-glycan structures (Figure 16). However, in other studies, recombinant IgA1 produced in CHO adherent cell lines contained around 50% sialylated N-glycans (Yoo et al., 2010). To understand this phenomenon, FBS was added to the media to revert the CHO-K1 cell back to adherent cells and analyze the N-glycan if the glycosylation will change into complex N-glycans. Indeed, as seen in Figure 23, the amount of high-mannosylated N-glycan was greatly reduced, and galactosylated and sialylated N-glycan

structures were increased. In addition, to ensure that only recombinant IgA1 N-glycans were analyzed, silver staining and western blotting were done to Ham's F12 media supplemented with 10% FBS. In Figure 24A, a band can be seen at the size close to HC however, there is no band in the LC size. Even if we can see the band, the concentration is low to affect the total N-glycan structure analysis. In addition, in Figure 24B, there were no bands seen in the elution fraction.

Discussion

Aggregation is an important quality attributes that can greatly affect the safety and efficacy of recombinant antibodies. In this study, recombinant IgA1 aggregation was seen in all recombinant IgA1 producing cell lines might be due to self-aggregation. The enhanced productivity of recombinant IgA1 compared to the nonadapted cell lines may be responsible for the rise in aggregated IgA1 since it can increase exposure to other IgA1s and form self-aggregates. A prior study converted Cys-471 to serine to significantly increase the amount of monomeric IgA (Xie et al., 2021). Additionally, the post-processing step may benefit from the addition of a mild disulfide bond reducing agent to help minimize the aggregation of recombinant IgA1. However, caution should be exercised while improving monomeric IgA1 production since this could potentially raise the likelihood of aggregation.

N-glycosylation and in some extent O-glycosylation is an important post-translation modification that can influence the protein's safety and efficacy. For this reason, knowing the N-glycan profile can improve the quality of recombinant proteins. In this study, the N-glycan structures of recombinant IgA1 produced in CHO-K1 suspension cells and disaccharide-adapted CHO-K1 suspension cells were analyzed using RP-HPLC and LC-MS/MS. The N-glycan structures found on recombinant IgA1 producing CHO-K1 suspension cell line are mostly high-mannosylated and a few galactosylated, fucosylated, and sialylated structures (Figure 16). This result is in contrast with previous study which reported that human serum IgA which contains more than 90% of sialylated N-glycan structures (Mattu et al., 1998). A previous study has reported that recombinant IgA produced in adherent CHO-K1 cells contains 50% sialylated N-glycan structures (Yoo et al., 2010). The reason for this is currently unclear. However, previous studies have shown that increasing specific productivity can lead to high-mannosylated structures in recombinant IgG production (Jimenez del Val et al., 2016; Zalai et al., 2016). Another study suggests that lambda light chain in IgG can increase high-

mannosylated structures (van Berkel et al., 2009). Increase in osmolarity has also resulted in increase of high-mannosylated N-glycan structure for recombinant IgG (Mastrangeli et al., 2020). However, in this study, there is little evidence that osmolarity has an impact on the N-glycan profile of recombinant IgA1, indicating that the N-glycosylation is unaffected by hyperosmolarity condition (Figure 16). In the case of sucrose-adapted IgA1 producing cell lines, little is known for why it contains higher levels of high-mannosylated N-glycan structures and fewer galactosylated structures. The type of disaccharides supplemented also have little effect on the N-glycan structures of recombinant IgA1. MGAT1 gene expression levels among the cell lines are indeed unchanged, as shown by the RT-qPCR results (Figure 21). Hence, the similarities between the high-mannosylated N-glycan structures discovered may be explained. Interestingly when serum was introduced to the nonadapted CHO-K1 suspension cells, the amount of high-mannosylated N-glycan structures decreased, and the amount of complex N-glycan structures increased compared when using the serum-free media (Figure 23). Unfortunately, because fetal bovine serum is a poorly defined mixture of several proteins and chemicals, it is challenging to identify the specific chemical that improved N-glycosylation. This is the first study that reported N-glycan structures of recombinant IgA1 produced in CHO-K1 suspension cells cultivated in serum-free medium.

N-glycosylation is a necessary PTM that affects some activities of IgA. One of which is the ability of galactosylated N-glycan structure to bind to asialoglycoprotein receptor for clearance of IgA in the serum (Basset et al., 1999b). In another study, IgA O-glycans with high levels of terminal N-acetylgalactosamine can increase binding to $CD4^+$ and $CD8^+$, which are found in patient with rheumatoid arthritis (Fortune et al., 1990). In addition, IgA binding to Fcα receptor I (FcαRI) is not affected by N-glycan found in the C_H2 (Gomes et al., 2008). Therefore, despite our result produced high mannosylated N-glycan structures, theoretically, it might still be able to activate effector functions. Another study suggests that terminal sialylated

N-glycan of IgA can suppress cell-surface attachment of influenza virus and other sialic acid binding virus (Maurer et al., 2018). Unfortunately, in this study, we collected the total N-glycan of the recombinant IgA1 which is both the C_H2 and the terminal N-glycans. In future studies, we suggest that it is better to separately analyze the N-glycan glycosylation site-independently to make a better profile. Further studies should be done such as gene expression analysis on the different glycosylation genes to explain why there are high levels of oligomannose N-glycan structures. Furthermore, additional information is needed on the different culture parameters such as pH, media composition, temperature, and others to fine tune the N-glycosylation in recombinant IgA produced in CHO-K1 cells.

O-glycan structures found in IgA are O-GalNAc structures. In this study, O-glycan profiles of recombinant IgA1 producing nonadapted CHO-K1 cell and disaccharide-adapted CHO-K1 cell lines were determined by RP-HPLC and LC-MS/MS. The O-glycan profile of nonadapted CHO-K1 cell line were only detected in one group of the triplicate samples. The reason for this might be the lower production of rIgA in nonadapted cell line. Another reason might be the activity or expression of O-glycosylation enzymes were lower compared to disaccharide-adapted cell lines. The result shows that only nonadapted cell lines contain GalGalNAc O-glycan structures that is not found in disaccharide-adapted cell lines (Table 5). According to the RT-qPCR data, the nonadapted cell lines exhibited decreased ST3Gal gene expression, which is necessary for sialic acid to bind to the galactose residue in O-glycans (Figure 21). Thus, this might be the reason for the presence of GalGalNAc structures. The O-glycan profile of disaccharide-adapted cell lines are either monosialylated or disialylated O-GalNAc structures. It is interesting to see if this increase in sialylation the effect of might be being cultured in hyperosmotic conditions. However, currently there are no other studies regarding the effects of culture conditions on the O-glycosylation of recombinant proteins especially the effects of osmotic pressure. Interestingly, O-glycan profile of recombinant IgA

from CHO cells contain more sialylated O-glycan compare with human serum IgA which contain only 24% sialylated O-glycan (Takahashi et al., 2012). In addition, O-glycan from CHO cells contain only these structures as there is very low expression of β1,6-*N*-acetylglucosaminyltransferase (GCNT1) in CHO cell which is necessary to elongate O-glycosylation structures to produce longer O-glycan structures (Liu et al., 2015). To the best of our knowledge, this is the first time that O-glycan profile of recombinant IgA were analyzed and changed based on adaptation on different disaccharides.

Currently, there are fewer studies on O-glycan compared to N-glycan because of the difficulty in determining the different structures and functions. However, based on the current observations on the purpose of O-glycan structures, several functions were elucidated such as supporting the extended structure of mucins and stem sections of membrane-bound proteins are their structural and modulatory functions, providing protection on the epithelial surface against pathogens, participating in receptor interactions, specifically adhesion for the binding and homing of immune cells, and safeguarding against endogenous cleaving enzymes to stop degradation and to direct and control the appropriate maturation of pro-proteins (Wandall et al., 2021). Indeed, there are several studies which elucidated some of the activities of O-glycan in IgA. One of these is the ability of IgA O-glycan to bind pathogens in the gut epithelium and bind ricin, with O-glycan terminal galactose (Arnold et al., 2007). A previous study discovered that IgA's O-glycan epitopes can interact with a wide range of bacterial adhesins (Royle et al., 2003). In addition to these studies, it is also observed that patients with IgA nephropathy have IgA O-glycan with only terminal GalNAc which can increase the chances of self-aggregation and in turn elicit antigenic response to form IgG-IgA complex (Suzuki & Novak, 2021). Additional studies such gene expression analysis of O-glycosylation related enzymes must be made to further explain the effects of different culture conditions on O-glycosylation and how to control them to provide better recombinant IgA in the future.

Summary

Quality attributes such as HMW aggregate, and glycosylation is important to be analyzed because both can affect the safety and efficacy of recombinant IgA1. In this study, we discovered that IgA1 aggregation exists in all cell lines. The HMW aggregation was also found in the intracellular fractions of maltose-adapted cell line while it was found in the extracellular fractions for the nonadapted cell line. The reason for this might be because of the high productivity of disaccharide-adapted cell lines thereby increasing exposure to other rIgAs inside the cells. In addition, This HMW aggregate might possibly because of self-aggregation by the cysteine residue found in the tailpiece. In addition, disulfide reducing agents can reduce the aggregates confirming the disulfide bond formation with other rIgAs. Glycosylation is an essential PTM that affects the quality and safety of recombinant antibodies. Therefore, analysis of the glycosylation profile will provide us valuable information that can help us improve the recombinant protein. In this study, N-glycan and O-glycan of recombinant IgA1 from CHO-K1 suspension cells were analyzed. In addition, recombinant IgA1 from disaccharide-adapted CHO-K1 suspension cells were also analyzed. High mannose structures were found to be the major N-glycan structures in all cell lines. Additionally, few structures of galactosylated, sialylated, fucosylated, and agalactosylated were also found. Interestingly, sucrose-adapted cell line has the most abundant high mannose structures among all cell lines and no sialylated structures were detected. This high mannose structures found among the cell lines. This is the first time that N-glycan profile of recombinant IgA1 produced in CHO-K1 suspension cells were analyzed. O-glycan structures were found to be different from nonadapted and disaccharide-adapted CHO-K1 suspension cell lines. Nonadapted cell line contains nonsialylated core1 mucin type structure which was not found in disaccharide-adapted cell lines while recombinant IgA1 produced from disaccharide-adapted cell lines contain monosialylated and disialylated core1 mucin type O-glycans. In addition, lactose-adapted cell

lines have mostly monosialylated structures. The identical high-mannosylated N-glycan profile among the cell lines may be explained by the same MGAT1 gene expression levels. In addition, sialyltransferase levels from the disaccharide-adapted cell lines were increase compared to the nonadapted cell line which might be the reason for the increase in monosialylated O-glycan structures. This is the first study on profiling the O-glycan of recombinant IgA1 produced on CHO-K1 suspension cells also the effects of media supplementation on the O-glycan. Further study is needed to understand metabolic changes that happens when media composition is changed such as the change in pH, the collection time of recombinant IgA1, and addition of glutathione and other productivity improving compounds.

Chapter 4 General Conclusions and Perspectives

Currently, IgG has been the major immunoglobulin backbone for recombinant antibody production due to being produced in substantial amount and being well-studied. However, IgA can potentially be the next immunoglobulin backbone that can be utilized in the future because of its special features such as the ability to form dimers and improve affinity and form secretory IgA to cross epithelial membrane that IgG cannot reach.

In this study, specific productivity was increased significantly by the supplementation and adaptation of the CHO-K1 suspension cells in different disaccharides namely, sucrose, maltose, lactose, and trehalose. Among these, maltose and trehalose-adaptation produced the highest productivity reaching 10.2 pg/cell/day and 10.0 pg/cell/day, respectively (Figure 11B). This productivity is 4.5-fold increase compared to non-adapted cell lines. Cultivation in hyperosmotic condition has been known to decrease cell growth rate and cell count and increase cell viability in extended periods. This extension of cell viability might have contributed to the increase in productivity. Indeed, previous studies have reported that recombinant protein production was the highest in the stationary phase compared to log phase (Templeton et al., 2013). A problem encountered in this study was the increase in aggregated IgA1. Hyperosmotic conditions can reduce antibody aggregation in IgG but increase aggregation in other recombinant proteins (Zhou et al., 2018). Also in this study, IgA aggregation was increase especially in disaccharide-adapted cell lines. However, the osmolarity is not the sole reason for the aggregation. The cysteine residue found on the terminal heavy chain can form self-aggregates with other IgA in the absence of the JC might be the cause (Xie et al., 2021). Indeed, aggregation was found in the intracellular fraction of maltose-adapted cell line which is a high productivity cell line while aggregation was found in the extracellular fraction of the nonadapted cell line. In addition, different reducing agents such as DTT, TCEP HCl, and glutathione has shown to reduce the IgA aggregates (Figure 15 A to D).

Although there is an increase in IgA aggregation in maltose-adapted cell line, the amount of IgA produced is still substantial compared to nonadapted cell lines.

Aside from the IgA productivity and aggregation analysis, N- and O-glycan profiling were also done in this study. N-glycan structures of nonadapted and disaccharide-adapted cell lines contain mostly of high-mannosylated structures. This result was found to be completely different from adherent IgA producing cell lines which contains mostly of complex N-glycan such as galactosylated N-glycan structures (Figure 23). Interestingly, the simple addition of fetal bovine serum can change the N-glycan profile of the recombinant IgA1. In addition, mRNA expression level of MGAT1 was analyzed in order to understand the N-glycan profile. Indeed, nonadapted and disaccharide-adapted cell lines express the same levels of MGAT1 which shows that hyperosmolarity does not affect N-glycosylation profiles. However, in the case of O-glycosylation, disaccharide-adapted cell lines produced more SiaGalGalNAc structures. Expression levels of the different sialyltransferases was measured and increase was seen in the disaccharide-adapted cell line compared to nonadapted cell line. To the best of our knowledge, this is the first time that O-glycosylation was shown to be affected by hyperosmotic conditions.

In general, this study deepened our understanding in recombinant antibody production particularly IgA1 in CHO-K1 suspension cells under hyperosmotic condition. The information here might serve as a useful guide for the future and foster the improvement of recombinant protein production technology.

Appendix

The O-glycosylation analysis is currently undergoing re-analysis to enhance data visualization for its upcoming publication.

Bibliography

Allen, A. C., Willis, F. R., Beattie, T. J., & Feehally, J. (1998). Abnormal IgA glycosylation in Henoch-Schönlein purpura restricted to patients with clinical nephritis. *Nephrology Dialysis Transplantation*, *13*(4), 930–934. https://doi.org/10.1093/NDT/13.4.930

Arnold, J. N., Wormald, M. R., Sim, R. B., Rudd, P. M., & Dwek, R. A. (2007). The impact of glycosylation on the biological function and structure of human immunoglobulins. *Annual Review of Immunology*, *25*(1), 21–50. https://doi.org/10.1146/annurev.immunol.25.022106.141702

Balu, S., Reljic, R., Lewis, M. J., Pleass, R. J., McIntosh, R., Kooten, C. van, Egmond, M. van, Challacombe, S., Woof, J. M., & Ivanyi, J. (2011). A novel human IgA monoclonal antibody protects against tuberculosis. *The Journal of Immunology*, *186*(5), 3113–3119. https://doi.org/10.4049/JIMMUNOL.1003189

Basset, C., Devauchelle, V., Durand, V., Jamin, C., Pennec, Y. L., Youinou, P., & Dueymes, M. (1999a). Glycosylation of immunoglobulin A influences its receptor binding. *Scandinavian Journal of Immunology*, *50*(6), 572–579. https://doi.org/10.1046/J.1365-3083.1999.00628.X

Basset, C., Devauchelle, V., Durand, V., Jamin, C., Pennec, Y. L., Youinou, P., & Dueymes, M. (1999b). Glycosylation of immunoglobulin A influences its receptor binding. *Scandinavian Journal of Immunology*, *50*(6), 572–579. https://doi.org/10.1046/J.1365-3083.1999.00628.X

Berger, M., Kaup, M., & Blanchard, V. (2011). Protein glycosylation and its impact on biotechnology. *Advances in Biochemical Engineering/Biotechnology*, *127*, 165–185. https://doi.org/10.1007/10_2011_101

Devudu Puligedda, R., Vigdorovich, V., Kouiavskaia, D., Kattala, C. D., Zhao, J.-Y., Al-Saleem, F. H., Chumakov, K., Sather, D. N., Dessain, S. K., Org, P., Org, K., & Org, A.-S. (2020). Human IgA monoclonal antibodies that neutralize poliovirus, produced by hybridomas and recombinant expression. *Antibodies 2020, Vol. 9, Page 5*, *9*(1), 5. https://doi.org/10.3390/ANTIB9010005

Ejemel, M., Li, Q., Hou, S., Schiller, Z. A., Tree, J. A., Wallace, A., Amcheslavsky, A., Kurt Yilmaz, N., Buttigieg, K. R., Elmore, M. J., Godwin, K., Coombes, N., Toomey, J. R., Schneider, R., Ramchetty, A. S., Close, B. J., Chen, D. Y., Conway, H. L., Saeed, M., … Wang, Y. (2020). A cross-reactive human IgA monoclonal antibody blocks SARS-CoV-2 spike-ACE2 interaction. *Nature Communications 2020 11:1*, *11*(1), 1–9. https://doi.org/10.1038/s41467-020-18058-8

Fortune, F., Kingston, J., Barnes, C. S., & Lehner, T. (1990). Identification and characterization of IgA and Vicia villosa-binding T cell subsets in rheumatoid arthritis. *Clin. Exp. Immunol*, *79*, 202–208.

Global Biotechnology - Industry Data, Trends, Stats | IBISWorld. (n.d.). Retrieved January 12, 2022, from https://www.ibisworld.com/global/market-research-reports/global-biotechnology-industry/

Gomes, M. M., Wall, S. B., Takahashi, K., Novak, J., Renfrow, M. B., & Herr, A. B. (2008). Analysis of IgA1 N-glycosylation and its contribution to FcαRI binding. *Biochemistry*, *47*(43), 11285–11299. https://doi.org/10.1021/BI801185B/SUPPL_FILE/BI801185B_SI_001.PDF

Göritzer, K., Maresch, D., Altmann, F., Obinger, C., & Strasser, R. (2017). Exploring site-Specific N-Glycosylation of HEK293 and plant-produced human IgA isotypes. *Journal of Proteome Research*, *16*(7), 2560–2570. https://doi.org/10.1021/ACS.JPROTEOME.7B00121/ASSET/IMAGES/LARGE/PR-2017-00121H_0007.JPEG

Haberger, M., Leiss, M., Heidenreich, A. K., Pester, O., Hafenmair, G., Hook, M., Bonnington, L., Wegele, H., Haindl, M., Reusch, D., & Bulau, P. (2016). Rapid characterization of biotherapeutic proteins by size-exclusion chromatography coupled to native mass spectrometry. *MAbs*, *8*(2), 331–339. https://doi.org/10.1080/19420862.2015.1122150/SUPPL_FILE/KMAB_A_1122150_SM8413.DOCX

Han, Y. K., Kim, Y. G., Kim, J. Y., & Lee, G. M. (2010). Hyperosmotic stress induces autophagy and apoptosis in recombinant Chinese hamster ovary cell culture. *Biotechnology and Bioengineering*, *105*(6), 1187–1192. https://doi.org/10.1002/BIT.22643

Hossler, P., Racicot, C., Chumsae, C., McDermott, S., & Cochran, K. (2017). Cell culture media supplementation of infrequently used sugars for the targeted shifting of protein glycosylation profiles. *Biotechnology Progress*, *33*(2), 511–522. https://doi.org/10.1002/BTPR.2429

Jenkins, N., Parekh, R. B., & James, D. C. (1996). Getting the glycosylation right: implications for the biotechnology industry. *Nature Biotechnology*, *14*(8), 975–981. https://doi.org/10.1038/NBT0896-975

Jimenez del Val, I., Fan, Y., & Weilguny, D. (2016). Dynamics of immature mAb glycoform secretion during CHO cell culture: An integrated modelling framework. *Biotechnology Journal*, *11*(5), 610–623. https://doi.org/10.1002/BIOT.201400663

Johansen, Braathen, & Brandtzaeg. (2000). Role of J chain in secretory immunoglobulin formation. *Scandinavian Journal of Immunology*, *52*(3), 240–248. https://doi.org/10.1046/J.1365-3083.2000.00790.X

Johansen, F.-E., Braathen, R., & Brandtzaeg, P. (2001). The J chain is essential for polymeric Ig receptor-mediated epithelial transport of IgA. *The Journal of Immunology*, *167*(9), 5185–5192. https://doi.org/10.4049/JIMMUNOL.167.9.5185

John Benson D. Choa, Tadahiro Sasaki, Hiroyuki Kajiura, Kazuyoshi Ikuta, Kazuhito Fujiyama, Ryo Misaki (2023). Effects of various disaccharide adaptations on recombinant IgA1 production in CHO-K1 suspension cells. *Cytotechnology*. DOI :10.1007/s10616-023-00571-5.

Kamachi, Y., & Omasa, T. (2018). Development of hyper osmotic resistant CHO host cells for enhanced antibody production. *Journal of Bioscience and Bioengineering*, *125*(4), 470–478. https://doi.org/10.1016/J.JBIOSC.2017.11.002

Kiehl, T. R., Shen, D., Khattak, S. F., Jian Li, Z., & Sharfstein, S. T. (2011). Observations of cell size dynamics under osmotic stress. *Cytometry Part A*, *79A*(7), 560–569. https://doi.org/10.1002/CYTO.A.21076

Kim, J. Y., Kim, Y. G., & Lee, G. M. (2012). Differential in-gel electrophoresis (DIGE) analysis of CHO cells under hyperosmotic pressure: Osmoprotective effect of glycine betaine addition. *Biotechnology and Bioengineering*, *109*(6), 1395–1403. https://doi.org/10.1002/BIT.24442

Kim, N. S., & Lee, G. M. (2002). Response of recombinant Chinese hamster ovary cells to hyperosmotic pressure: effect of Bcl-2 overexpression. *Journal of Biotechnology*, *95*(3), 237–248. https://doi.org/10.1016/S0168-1656(02)00011-1

Kunert, R., & Reinhart, D. (2016). Advances in recombinant antibody manufacturing. *Applied Microbiology and Biotechnology*, *100*(8), 3451–3461. https://doi.org/10.1007/S00253-016-7388-9/FIGURES/3

Lao, M. S., & Toth, D. (1997). Effects of ammonium and lactate on growth and metabolism of a recombinant Chinese hamster ovary cell culture. *Biotechnology Progress*, *13*(5), 688–691. https://doi.org/10.1021/BP9602360

Lee, M. S., Kim, K. W., Kim, Y. H., & Lee, G. M. (2003). Proteome analysis of antibody-expressing CHO cells in response to hyperosmotic pressure. *Biotechnology Progress*, *19*(6), 1734–1741. https://doi.org/10.1021/BP034093A

Leong, D. S. Z., Tan, J. G. L., Chin, C. L., Mak, S. Y., Ho, Y. S., & Ng, S. K. (2017). Evaluation and use of disaccharides as energy source in protein-free mammalian cell cultures. *Scientific Reports 2017 7:1*, *7*(1), 1–10. https://doi.org/10.1038/srep45216

Leong, D. S. Z., Teo, B. K. H., Tan, J. G. L., Kamari, H., Yang, Y. S., Zhang, P., & Ng, S. K. (2018). Application of maltose as energy source in protein-free CHO-K1 culture to improve the production of recombinant monoclonal antibody. *Scientific Reports 2018 8:1*, *8*(1), 1–12. https://doi.org/10.1038/s41598-018-22490-8

Leusen, J. H. W. (2015). IgA as therapeutic antibody. *Molecular Immunology*, *68*(1), 35–39. https://doi.org/10.1016/J.MOLIMM.2015.09.005

Liu, J., Jin, C., Cherian, R. M., Karlsson, N. G., & Holgersson, J. (2015). O-glycan repertoires on a mucin-type reporter protein expressed in CHO cell pools transiently transfected with O-glycan core enzyme cDNAs. *Journal of Biotechnology*, *199*, 77–89. https://doi.org/10.1016/J.JBIOTEC.2015.02.017

Lohse, S., Derer, S., Beyer, T., Klausz, K., Peipp, M., Leusen, J. H. W., Winkel, J. G. J. van de, Dechant, M., & Valerius, T. (2011). Recombinant dimeric IgA antibodies against the epidermal growth factor receptor mediate effective tumor cell killing. *The Journal of Immunology*, *186*(6), 3770–3778. https://doi.org/10.4049/JIMMUNOL.1003082

Marth, J. D., & Grewal, P. K. (2008). Mammalian glycosylation in immunity. *Nature Reviews Immunology 2008 8:11*, *8*(11), 874–887. https://doi.org/10.1038/nri2417

Mastrangeli, R., Audino, M. C., Palinsky, W., Broly, H., & Bierau, H. (2020). The formidable challenge of controlling high mannose-type N-glycans in therapeutic mAbs. *Trends in Biotechnology*, *38*(10), 1154–1168. https://doi.org/10.1016/J.TIBTECH.2020.05.009

Matsumoto, M. L. (2022). Molecular mechanisms of multimeric assembly of IgM and IgA. *Https://Doi.Org/10.1146/Annurev-Immunol-101320-123742*, *40*(1). https://doi.org/10.1146/ANNUREV-IMMUNOL-101320-123742

Mattu, T. S., Pleass, R. J., Willis, A. C., Kilian, M., Wormald, M. R., Lellouch, A. C., Rudd, P. M., Woof, J. M., & Dwek, R. A. (1998). The glycosylation and structure of human serum IgA1, Fab, and Fc regions and the role of N-glycosylation on Fcα receptor interactions. *Journal of Biological Chemistry*, *273*(4), 2260–2272. https://doi.org/10.1074/jbc.273.4.2260

Maurer, M. A., Meyer, L., Bianchi, M., Turner, H. L., Le, N. P. L., Steck, M., Wyrzucki, A., Orlowski, V., Ward, A. B., Crispin, M., & Hangartner, L. (2018). Glycosylation of human IgA directly inhibits Influenza A and other sialic-acid-binding viruses. *Cell Reports*, *23*(1), 90–99. https://doi.org/10.1016/J.CELREP.2018.03.027

Moreira, J. da V., de Staercke, L., Martínez-Basilio, P. C., Gauthier-Thibodeau, S., Montégut, L., Schwartz, L., & Jolicoeur, M. (2021). Hyperosmolarity triggers the warburg effect in Chinese hamster ovary cells and reveals a reduced mitochondria horsepower. *Metabolites 2021, Vol. 11, Page 344*, *11*(6), 344. https://doi.org/10.3390/METABO11060344

Mullard, A. (2021). 2020 FDA drug approvals. *Nature Reviews. Drug Discovery*, *20*(2), 85–90. https://doi.org/10.1038/D41573-021-00002-0

Nakanishi, K., Morikane, S., Ichikawa, S., Kurohane, K., Niwa, Y., Akimoto, Y., Matsubara, S., Kawakami, H., Kobayashi, H., & Imai, Y. (2017). Protection of human colon cells from Shiga toxin by plant-based recombinant secretory IgA. *Scientific Reports 2017 7:1*, *7*(1), 1–12. https://doi.org/10.1038/srep45843

Novak, J., Julian, B. A., Mestecky, J., & Renfrow, M. B. (2012). Glycosylation of IgA1 and pathogenesis of IgA nephropathy. *Seminars in Immunopathology 2012 34:3*, *34*(3), 365–382. https://doi.org/10.1007/S00281-012-0306-Z

Oh, S. K. W., Vig, P., Chua, F., Teo, W. K., & Yap, M. G. S. (1993). Substantial overproduction of antibodies by applying osmotic pressure and sodium butyrate. *Biotechnology and Bioengineering*, *42*(5), 601–610. https://doi.org/10.1002/BIT.260420508

Onitsuka, M., Tatsuzawa, M., Asano, R., Kumagai, I., Shirai, A., Maseda, H., & Omasa, T. (2014). Trehalose suppresses antibody aggregation during the culture of Chinese hamster ovary cells. *Journal of Bioscience and Bioengineering*, *117*(5), 632–638. https://doi.org/10.1016/J.JBIOSC.2013.10.022

Ozturk, S. S., Riley, M. R., & Palsson, B. O. (1992). Effects of ammonia and lactate on hybridoma growth, metabolism, and antibody production. *Biotechnology and Bioengineering*, *39*(4), 418–431. https://doi.org/10.1002/BIT.260390408

Paul, M., & Ma, J. K. C. (2011). Plant-made pharmaceuticals: leading products and production platforms. *Biotechnology and Applied Biochemistry*, *58*(1), 58–67. https://doi.org/10.1002/BAB.6

Pecetta, S., Finco, O., & Seubert, A. (2020). Quantum leap of monoclonal antibody (mAb) discovery and development in the COVID-19 era. *Seminars in Immunology*, *50*, 101427. https://doi.org/10.1016/J.SMIM.2020.101427

Pfizenmaier, J., Junghans, L., Teleki, A., & Takors, R. (2016). Hyperosmotic stimulus study discloses benefits in ATP supply and reveals miRNA/mRNA targets to improve recombinant protein production of CHO cells. *Biotechnology Journal*, *11*(8), 1037–1047. https://doi.org/10.1002/BIOT.201500606

Qin, J., Wu, X., Xia, Z., Huang, Z., Zhang, Y., Wang, Y., Fu, Q., & Zheng, C. (2019). The effect of hyperosmolality application time on production, quality, and biopotency of monoclonal antibodies produced in CHO cell fed-batch and perfusion cultures. *Applied Microbiology and Biotechnology*, *103*(3), 1217–1229. https://doi.org/10.1007/S00253-018-9555-7/FIGURES/9

Reinhart, D., & Kunert, R. (2015). Upstream and downstream processing of recombinant IgA. *Biotechnology Letters*, *37*(2), 241–251. https://doi.org/10.1007/S10529-014-1686-Z/TABLES/2

Rish, A. J., Drennen, J. K., & Anderson, C. A. (2022). Metabolic trends of Chinese hamster ovary cells in biopharmaceutical production under batch and fed-batch conditions. *Biotechnology Progress*, *38*(1), e3220. https://doi.org/10.1002/BTPR.3220

Ritacco, F. v., Wu, Y., & Khetan, A. (2018). Cell culture media for recombinant protein expression in Chinese hamster ovary (CHO) cells: History, key components, and optimization strategies. *Biotechnology Progress*, *34*(6), 1407–1426. https://doi.org/10.1002/BTPR.2706

Romanova, N., Niemann, T., Greiner, J. F. W., Kaltschmidt, B., Kaltschmidt, C., & Noll, T. (2021). Hyperosmolality in CHO culture: Effects on cellular behavior and morphology. *Biotechnology and Bioengineering*, *118*(6), 2348–2359. https://doi.org/10.1002/BIT.27747

Romanova, N., Schelletter, L., Hoffrogge, R., & Noll, T. (2022). Hyperosmolality in CHO cell culture: effects on the proteome. *Applied Microbiology and Biotechnology*, *106*(7), 2569–2586. https://doi.org/10.1007/S00253-022-11861-X/FIGURES/5

Rosenberg, A. S. (2006). Effects of protein aggregates: An immunologic perspective. *The AAPS Journal*, *8*(3), E501. https://doi.org/10.1208/AAPSJ080359

Royle, L., Roos, A., Harvey, D. J., Wormald, M. R., van Gijlswijk-Janssen, D., Redwan, E. R. M., Wilson, I. A., Daha, M. R., Dwek, R. A., & Rudd, P. M. (2003). Secretory IgA N- and O-glycans provide a link between the innate and adaptive immune systems. *The Journal of Biological Chemistry*, *278*(22), 20140–20153. https://doi.org/10.1074/JBC.M301436200

Rudd, P. M., & Dwek, R. A. (2000). Determining the structure of oligosaccharides N- and O-linked to glycoproteins. *Current Protocols in Protein Science*, *22*(1), 12.6.1-12.6.47. https://doi.org/10.1002/0471140864.PS1206S22

Sano, K., Saito, S., Suzuki, T., Kotani, O., Ainai, A., van Riet, E., Tabata, K., Saito, K., Takahashi, Y., Yokoyama, M., Sato, H., Maruno, T., Usami, K., Uchiyama, S., Ogawa-Goto, K., & Hasegawa, H. (2021). An influenza HA stalk reactive polymeric IgA antibody exhibits anti-viral function regulated by binary interaction between HA and the antibody. *PLOS ONE*, *16*(1), e0245244. https://doi.org/10.1371/JOURNAL.PONE.0245244

Sasaki, T., Setthapramote, C., Kurosu, T., Nishimura, M., Asai, A., Omokoko, M. D., Pipattanaboon, C., Pitaksajjakul, P., Limkittikul, K., Subchareon, A., Chaichana, P., Okabayashi, T., Hirai, I., Leaungwutiwong, P., Misaki, R., Fujiyama, K., Ono, K. ichiro, Okuno, Y., Ramasoota, P., & Ikuta, K. (2013). Dengue virus neutralization and antibody-dependent enhancement activities of human monoclonal antibodies derived from dengue patients at acute phase of secondary infection. *Antiviral Research*, *98*(3), 423–431. https://doi.org/10.1016/J.ANTIVIRAL.2013.03.018

Schiestl, M., Stangler, T., Torella, C., Čepeljnik, T., Toll, H., & Grau, R. (2011). Acceptable changes in quality attributes of glycosylated biopharmaceuticals. *Nature Biotechnology 2011 29:4*, *29*(4), 310–312. https://doi.org/10.1038/nbt.1839

Seibert, C. W., Rahmat, S., Krause, J. C., Eggink, D., Albrecht, R. A., Goff, P. H., Krammer, F., Duty, J. A., Bouvier, N. M., Garcia-Sastre, A., & Palese, P. (2013). Recombinant IgA is sufficient to prevent Influenza virus transmission in Guinea pigs. *Journal of Virology*, *87*(14), 7793–7804. https://doi.org/10.1128/JVI.00979-13/ASSET/AFB60A92-A438-4A67-B65C-43B560F00ADA/ASSETS/GRAPHIC/ZJV9990978730006.JPEG

Sousa-Pereira, P. de, & Woof, J. M. (2019). IgA: structure, function, and developability. *Antibodies 2019, Vol. 8, Page 57*, *8*(4), 57. https://doi.org/10.3390/ANTIB8040057

Steffen, U., Koeleman, C. A., Sokolova, M. v., Bang, H., Kleyer, A., Rech, J., Unterweger, H., Schicht, M., Garreis, F., Hahn, J., Andes, F. T., Hartmann, F., Hahn, M., Mahajan, A., Paulsen, F., Hoffmann, M., Lochnit, G., Muñoz, L. E., Wuhrer, M., … Schett, G. (2020). IgA subclasses have different effector functions associated with distinct glycosylation profiles. *Nature Communications 2020 11:1*, *11*(1), 1–12. https://doi.org/10.1038/s41467-019-13992-8

Sun, L. K., Fung, M. S. C., Sun, W. N. C., Sun, C. R. Y., Chang, W. I., & Chang, T. W. (1995). Human IgA monoclonal antibodies specific for a major ragweed pollen antigen. *Bio/Technology 1995 13:8*, *13*(8), 779–786. https://doi.org/10.1038/nbt0895-779

Suzuki, H., & Novak, J. (2021). IgA glycosylation and immune complex formation in IgAN. *Seminars in Immunopathology*, *43*(5), 669–678. https://doi.org/10.1007/S00281-021-00883-8/FIGURES/2

Takahashi, K., Smith, A. D., Poulsen, K., Kilian, M., Julian, B. A., Mestecky, J., Novak, J., & Renfrow, M. B. (2012). Naturally occurring structural isomers in serum IgA1 O -glycosylation. *Journal of Proteome Research*, *11*(2), 692–702. https://doi.org/10.1021/PR200608Q/SUPPL_FILE/PR200608Q_SI_001.PDF

Templeton, N., Dean, J., Reddy, P., & Young, J. D. (2013). Peak antibody production is associated with increased oxidative metabolism in an industrially relevant fed-batch CHO cell culture. *Biotechnology and Bioengineering*, *110*(7), 2013–2024. https://doi.org/10.1002/BIT.24858

Tihanyi, B., & Nyitray, L. (2020). Recent advances in CHO cell line development for recombinant protein production. *Drug Discovery Today: Technologies*, *38*, 25–34. https://doi.org/10.1016/J.DDTEC.2021.02.003

Tissandié, E., Morelle, W., Berthelot, L., Vrtovsnik, F., Daugas, E., Walker, F., Lebrec, D., Trawalé, J. M., Francoz, C., Durand, F., Moura, I. C., Paradis, V., Moreau, R., & Monteiro, R. C. (2011). Both IgA nephropathy and alcoholic cirrhosis feature abnormally glycosylated IgA1 and soluble CD89–IgA and IgG–IgA complexes: common mechanisms for distinct diseases. *Kidney International*, *80*(12), 1352–1363. https://doi.org/10.1038/KI.2011.276

van Berkel, P. H. C., Gerritsen, J., Perdok, G., Valbjørn, J., Vink, T., van de Winkel, J. G. J., & Parren, P. W. H. I. (2009). N-linked glycosylation is an important parameter for optimal selection of cell lines producing biopharmaceutical human IgG. *Biotechnology Progress*, *25*(1), 244–251. https://doi.org/10.1002/BTPR.92

Virdi, V., Juarez, P., Boudolf, V., & Depicker, A. (2016). Recombinant IgA production for mucosal passive immunization, advancing beyond the hurdles. *Cellular and Molecular Life Sciences*, *73*(3), 535–545. https://doi.org/10.1007/S00018-015-2074-0/TABLES/1

Walsh, G., & Walsh, E. (2022). Biopharmaceutical benchmarks 2022. *Nature Biotechnology 2022 40:12*, *40*(12), 1722–1760. https://doi.org/10.1038/s41587-022-01582-x

Wandall, H. H., Nielsen, M. A. I., King-Smith, S., de Haan, N., & Bagdonaite, I. (2021). Global functions of O-glycosylation: promises and challenges in O-glycobiology. *The FEBS Journal*, *288*(24), 7183–7212. https://doi.org/10.1111/FEBS.16148

Woof, J. M., & Ken, M. A. (2006). The function of immunoglobulin A in immunity. *The Journal of Pathology*, *208*(2), 270–282. https://doi.org/10.1002/PATH.1877

Woof, J. M., & Russell, M. W. (2011). Structure and function relationships in IgA. *Mucosal Immunology 2011 4:6*, *4*(6), 590–597. https://doi.org/10.1038/mi.2011.39

Wormald, M. R., & Sim, R. B. (2007). *The Impact of Glycosylation on the Biological Function and Structure of Human Immunoglobulins Article in Annual Review of Immunology ·*. https://doi.org/10.1146/annurev.immunol.25.022106.141702

Xie, X., Gao, L., Liu, P., Lv, J., Lu, W. H., Zhang, H., & Jin, J. (2021). Propensity of IgA to self-aggregate via tailpiece cysteine-471 and treatment of IgA nephropathy using cysteamine. *JCI Insight*, *6*(19). https://doi.org/10.1172/JCI.INSIGHT.150551

Xu, T., Zhang, J., Wang, T., & Wang, X. (2022). Recombinant antibodies aggregation and overcoming strategies in CHO cells. *Applied Microbiology and Biotechnology*, *106*(11), 3913–3922. https://doi.org/10.1007/S00253-022-11977-0/METRICS

Yoo, E. M., Yu, L. J., Wims, L. A., Goldberg, D., & Morrison, S. L. (2010). Differences in N-glycan structures found on recombinant IgA1 and IgA2 produced in murine myeloma and CHO cell lines. *Https://Doi.Org/10.4161/Mabs.2.3.11802*, *2*(3), 320–334. https://doi.org/10.4161/MABS.2.3.11802

Zalai, D., Hevér, H., Lovász, K., Molnár, D., Wechselberger, P., Hofer, A., Párta, L., Putics, Á., & Herwig, C. (2016). A control strategy to investigate the relationship between specific productivity and high-mannose glycoforms in CHO cells. *Applied Microbiology and Biotechnology*, *100*(16), 7011–7024. https://doi.org/10.1007/S00253-016-7380-4/FIGURES/9

Zhang, X., Garcia, I. F., Baldi, L., Hacker, D. L., & Wurm, F. M. (2010). Hyperosmolarity enhances transient recombinant protein yield in Chinese hamster ovary cells. *Biotechnology Letters*, *32*(11), 1587–1592. https://doi.org/10.1007/S10529-010-0331-8/FIGURES/4

Zhou, Y., Raju, R., Alves, C., & Gilbert, A. (2018). Debottlenecking protein secretion and reducing protein aggregation in the cellular host. *Current Opinion in Biotechnology*, *53*, 151–157. https://doi.org/10.1016/J.COPBIO.2018.01.007

List of Publication

John Benson D. Choa, Tadahiro Sasaki, Hiroyuki Kajiura, Kazuyoshi Ikuta, Kazuhito Fujiyama, Ryo Misaki. Effects of various disaccharide adaptations on recombinant IgA1 production in CHO-K1 suspension cells. Cytotechnology. 2023. DOI :10.1007/s10616-023-00571-5.

Acknowledgement

I am deeply grateful to Prof. Kazuhito Fujiyama for his invaluable guidance and support throughout the course of this research, which would not have been possible without his expertise, patience, and encouragement. I would also like to thank Dr. Ryo Misaki for his unwavering support and encouragement throughout this journey, as well as for his critical guidance and knowledge that helped me complete my study. Lastly, I am thankful for the invaluable comments provided by Dr. Hiroyuki Kajiura, which greatly improved my dissertation, presentation, and publication.

I would like to thank Prof. Takeshi Omasa and Prof. Susumu Uchiyama, my review committee, who lend their expertise to greatly improve my presentation and dissertation.

I would like to express my appreciation to the Japanese Government, particularly the Ministry of Education, Culture, Sports, Science and Technology (MEXT), for their support that made my study and living in Japan possible.

I would like to express my gratitude to ICBiotech staffs and my laboratory mates especially Aaron, Nicole, Ue, Doogi, Dua and others. For supporting and cheering me until the end.

I would like to express my gratitude to a few individuals who have made a significant impact in my life. Dr. Kevin Stapleton, a dear friend who taught me the importance of keeping an open mind and embracing life's complexities, rather than viewing everything in black and white. Secondly, I cannot imagine my life without Dr. Nara Quintela Begnini, whose unwavering support and camaraderie has been a guiding light, even during the darkest of days. Her presence has always made even the most challenging moments bright.

I would like to extend my heartfelt gratitude to my family, Juanito Choa, Margarita Choa, Joanna Marie Choa, and John Brian Choa, who have been my constant support system, even though we are miles apart.